



JRC SCIENCE FOR POLICY REPORT

Arctic permafrost thawing

*Impacts on high latitude
emissions of carbon dioxide
and methane*

Dobricic, S.

Pozzoli, L.

2019



This publication is a Science for Policy report by the Joint Research Centre (JRC), the European Commission's science and knowledge service. It aims to provide evidence-based scientific support to the European policymaking process. The scientific output expressed does not imply a policy position of the European Commission. Neither the European Commission nor any person acting on behalf of the Commission is responsible for the use that might be made of this publication. For information on the methodology and quality underlying the data used in this publication for which the source is neither Eurostat nor other Commission services, users should contact the referenced source. The designations employed and the presentation of material on the maps do not imply the expression of any opinion whatsoever on the part of the European Union concerning the legal status of any country, territory, city or area or of its authorities, or concerning the delimitation of its frontiers or boundaries.

Contact information

Name: Srdan Dobricic

Address: European Commission, Joint Research Centre, Directorate C: Energy, Transport and Climate, Air and Climate Unit, via E. Fermi 2749, 21027 Ispra - Italy

Email: srdan.dobricic@ec.europa.eu

Tel.: +39 0332 786376

EU Science Hub

<https://ec.europa.eu/jrc>

JRC109379

EUR 29940 EN

PDF	ISBN 978-92-76-10182-6	ISSN 1831-9424	doi:10.2760/007066
Print	ISBN 978-92-76-10201-4	ISSN 1018-5593	doi:10.2760/83312

Luxembourg: Publications Office of the European Union, 2019

© European Union, 2019



The reuse policy of the European Commission is implemented by the Commission Decision 2011/833/EU of 12 December 2011 on the reuse of Commission documents (OJ L 330, 14.12.2011, p. 39). Except otherwise noted, the reuse of this document is authorised under the Creative Commons Attribution 4.0 International (CC BY 4.0) licence (<https://creativecommons.org/licenses/by/4.0/>). This means that reuse is allowed provided appropriate credit is given and any changes are indicated. For any use or reproduction of photos or other material that is not owned by the EU, permission must be sought directly from the copyright holders.

All content © European Union, 2019.

How to cite this report: Dobricic, S. and Pozzoli, L., *Arctic permafrost thawing*, EUR 29940 EN, Publications Office of the European Union, Luxembourg, 2019, ISBN 978-92-76-10182-6, doi:10.2760/007066, JRC109379.

Contents

Acknowledgements	1
Executive summary	2
1 Introduction.....	3
2 Current and future temperature increase in the Arctic	8
2.1 Current near-surface temperature trends.....	8
2.2 Future near-surface temperature trends	10
3 Potential for methane and carbon dioxide release from permafrost thawing.....	14
3.1 Present and future carbon availability in unfrozen soils.....	14
3.2 Carbon dioxide emissions from microbial degradation.....	18
3.3 Methane emissions from boreal wetlands	20
3.4 Methane emissions from the Arctic Ocean.....	23
4 Impact of permafrost degradation on infrastructures.....	24
5 Conclusions	26
References	28
List of abbreviations and definitions	31
List of boxes.....	32
List of figures	33
List of tables.....	35
Annexes	36
Annex 1. Supplementary figures.....	36

Acknowledgements

We would like to thank the reviewers of this report Thomas Diehl, Peter Bergamaschi, Peeter Part, and Frederic Bastide.

Authors

Srdan Dobricic and Luca Pozzoli (European Commission, Joint Research Centre, Directorate C: Energy, Transport and Climate)

Executive summary

The strong amplification of global warming in the Arctic accelerates the rate of thawing of permafrost. This process could produce a positive feedback on global warming by emitting carbon into the atmosphere in the form of methane (CH₄) and carbon dioxide (CO₂). The EC and EEAS Joint communication to the European Parliament and the Council "An integrated European Union policy for the Arctic", and also the EU Global Strategy, call for the analysis and adaptation to large environmental changes in the Arctic permafrost. This report therefore evaluates the ongoing and future warming over the Arctic permafrost. It estimates the permafrost thawing rate and current and future emissions of CO₂ and CH₄ from the carbon deposit stored in the permafrost.

By using atmospheric model simulations of the last decades constrained by observations, i.e. atmospheric reanalysis, the report shows that Arctic amplification of global warming in the last decades is mainly due to warming over ocean and sea-ice in winter and over land in summer. During the last decades there are no significant positive trends of near-surface temperatures over land in winter. In the last decades summer trends of near-surface temperature over land in the Arctic are positive and similar to trends over global land areas.

When permafrost thaws its carbon content becomes available for microbial degradation and it is released into the atmosphere in the form of CO₂ and CH₄. It is found that total CO₂ emissions in the 21st century will not differ significantly between different RCP scenarios, because in all scenarios a large portion of carbon stored in the permafrost will become available for degradation by microbes. Current anthropogenic CO₂ emissions are at least ten times higher than emissions from the thawing permafrost. On the other hand, the reduction of global warming envisaged by the Paris agreement will require diminishing of anthropogenic emissions already in the first half of the 21st century. In this case future CO₂ emissions from the permafrost may become comparable to anthropogenic emissions and Paris agreement targets to reduce the global warming may be exceeded sooner than expected. The quota of CO₂ that humankind can emit to keep below the agreed level of global warming will likely diminish and additional efforts for achieving Paris Agreement goals will be required.

The literature review indicates that in the 21st century methane emissions from current permafrost areas over the land and Arctic Ocean will likely double or be several times higher than ongoing emissions. Although the warming potential of methane is much higher than the warming potential of CO₂, most of current estimates of future methane emissions indicate less significant impacts on global warming than those from CO₂. Eventual large emissions from methane hydrates stored at the Arctic Ocean bottom or sudden large CH₄ releases from permafrost in the 21st century are very difficult to predict, but they might more significantly impact the global warming rate.

Furthermore, thawing of permafrost endangers ecosystems and infrastructures at the local and regional scale, impacting local communities by limiting resource development and fragmenting ecosystems. Understanding of local processes with a sufficient spatial and temporal coverage will require a combination of field studies, remote sensing analysis and modelling approaches.

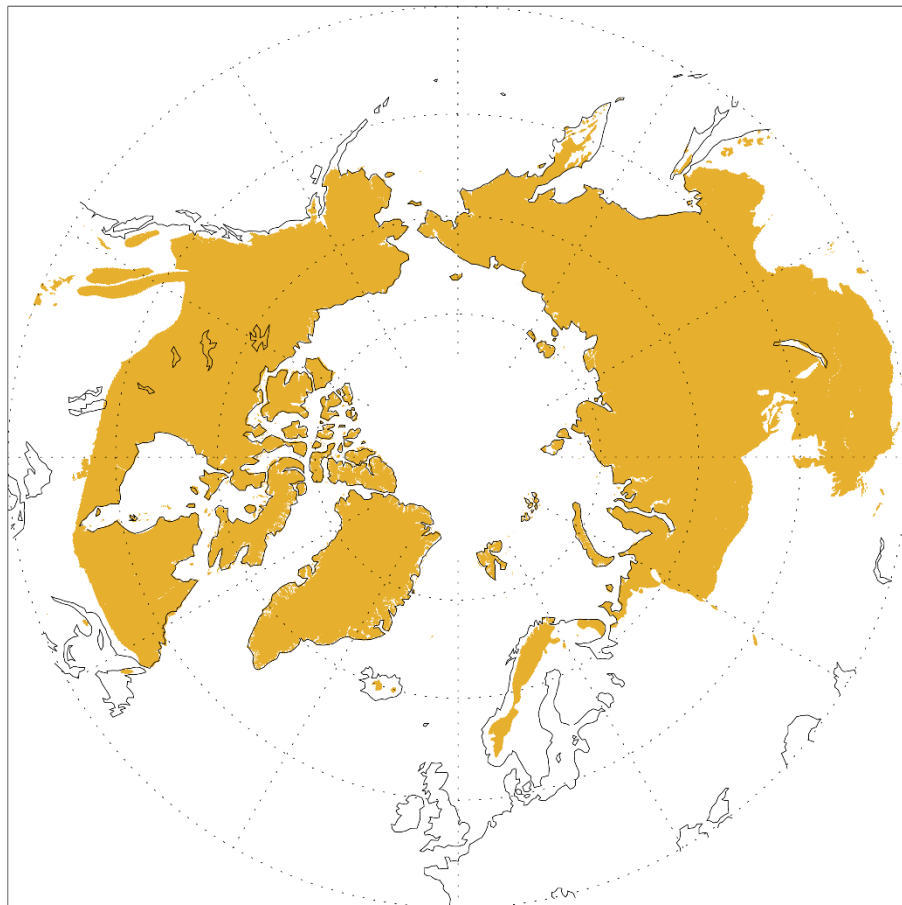
The results of this report may support the EU policy for the Arctic by providing additional evidence on the changing Arctic permafrost and presenting the range of estimates for emissions of CO₂ and CH₄ in the 21st century. The results may also provide a scientific contribution to the EU efforts in implementing the Paris agreement goals. In particular, they may support the EU science policy in the Arctic by emphasizing the need for the long term monitoring and predicting of permafrost thawing and its emissions of greenhouse gasses, in order to reduce the currently large uncertainties in estimating future impacts of permafrost thawing on climate change. In the future the methodology for estimating emissions of greenhouse gasses from the thawing permafrost developed in the report may be used with new scientific estimates of the emission rates and different climate scenarios including those that are more stringent than the Paris agreement.

1 Introduction

Permafrost is defined as the ground having layers with temperatures continuously below the freezing point for two or more consecutive years. Permafrost is usually formed below the ground surface. It may exist in northern latitudes, alpine regions, and polar coastal areas below ocean surface. Over land it typically forms when yearly averaged atmospheric temperatures are lower than the freezing point. If yearly averaged temperatures are close to the freezing point permafrost typically forms discontinuously into the sporadic permafrost. When yearly averaged temperatures are significantly lower than the freezing point, the discontinuous permafrost covers a larger fraction of the ground and at yearly averaged temperatures of -15°C permafrost typically becomes continuous.

In the Northern Hemisphere permafrost covers about one quarter of land surface. It is mostly present at northern latitudes, inland in areas distant from the influence from oceans and at high elevations following the 0°C isotherm of near-surface atmospheric temperatures. In Siberia and Canada permafrost surrounding the Arctic may extend southward to 50°N (Fig. 1). The permafrost coverage also varies from sporadic at lower latitudes to continuous in the Arctic (e.g. AMAP 2015).

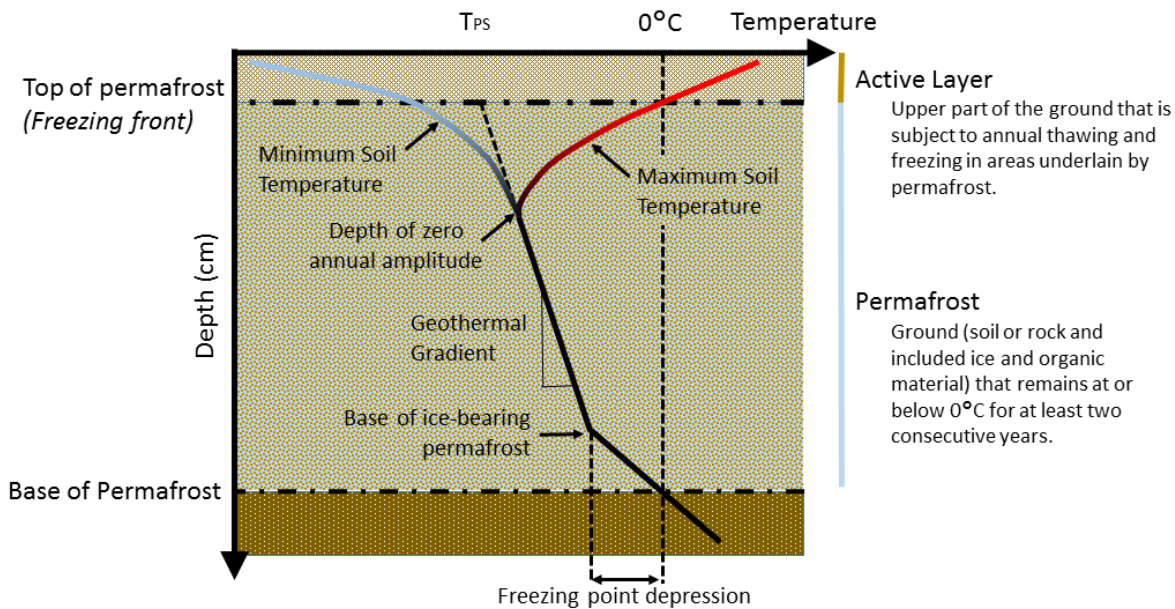
Figure 1. Land area covered by permafrost north of 45°N based on data from Hugelius et al (2014).



In summer, close to the surface, permafrost temperature may become higher than 0°C . The active layer is defined as the depth at which temperatures above the freezing point extend into the ground. They further warm frozen layers until reaching the depth at which temperatures become practically unchanged. Further in deep layers the geothermal warming limits the expansion of the frozen layer (Fig. 2). The sketch shows the annual minimum and maximum temperatures, which meet at the depth of zero annual amplitude, and continue following a common profile in the ground, with a linear geothermal gradient. A change in slope of the temperature profile occurs at the base of ice-bearing permafrost, which is caused by the difference in the thermal conductivities between frozen and unfrozen ground, at the base of permafrost. The annual mean

permafrost surface temperature, TPS, is defined extrapolating the temperature profile with a linear geothermal gradient upward.

Figure 2. Schematic representation of vertical temperature profiles of permafrost layers (the figure is an adaptation from Figure 1 of Osterkamp and Burn, 2003).



Permafrost extension and its thermal properties dynamically change with time. The main driver of permafrost extension and depth is the atmospheric temperature. Locally permafrost evolution may be influenced by snow cover, organic content in the soil, vegetation at the surface, soil moisture and drainage properties of the ground. These local conditions may change heat propagation in the ground and modify effects of atmospheric temperature on permafrost variability (e.g. AMAP 2015).

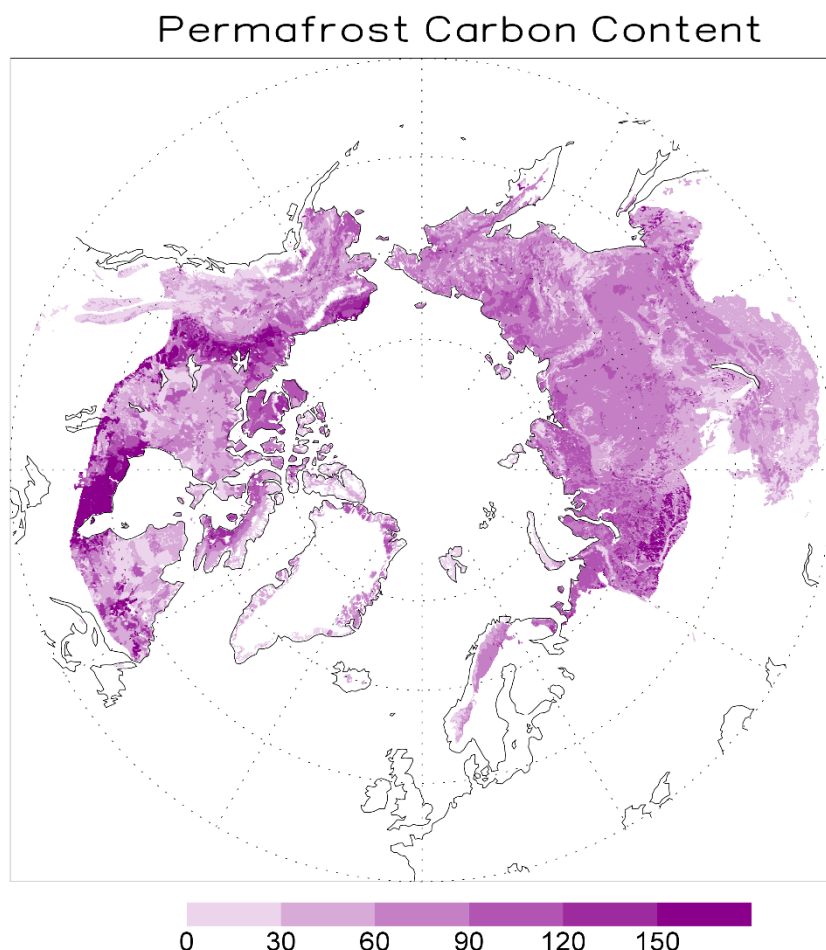
Box 1. Permafrost and estimated carbon content in frozen soil

In the past permafrost extension and thickness have experienced large changes. Permafrost was formed during periods of cold climate. Conditions for its formation became possible with climate cooling starting 40 million years ago (Schuur et al. 2015). About 20 thousand years ago, during the last glacial maximum, a thick layer of permafrost formed over land areas of North America, Asia and Europe. In this period, when the sea level was more than 100 m lower than today, permafrost also developed over continental shelf areas of the Arctic Ocean (Schuur et al. 2015). Subsequently, during the late Pleistocene and Holocene epochs it became submerged under the sea water. Since then permafrost extension was reduced to current levels. During the cold period between 1600 and 1850 shallow permafrost occurred in some areas, but since 1850 permafrost warms and is generally reduced in the northern Hemisphere (e.g. Schuur et al. 2015).

Past changes in climatic conditions over the permafrost area resulted in accumulation of deposited vegetation creating large concentration of organic carbon in the soil. It is estimated that near the surface (i.e. the three meters deep soil layer) the Arctic permafrost contains 1035 Pg (1 Pg = 109 tonnes) of carbon with the 95% confidence interval of 150 Pg (Schuur et al 2015). Fig. 3 shows the distribution of carbon content above 3 m depth over land obtained from the dataset by Hugelius et al. (2014).

During the last Ice Age significant deposits of organic carbon in the soil, named yedoma, are also accumulated below 3 m depth in Siberia and Alaska with mass estimated to vary between 210 and 450 Pg. It is further estimated that in the Arctic additional 350-450 Pg of organic carbon may be stored between 3 and 10 m depths outside of the yedoma region. Carbon content estimates over the costal shelf of the Arctic Ocean are very uncertain and largely unquantified. Although during the last Ice age 2.5 times larger permafrost area had been probably formed over the Arctic Ocean than over the yedoma region, sea water that subsequently covered the continental shelf maintained temperatures at the soil surface above the freezing level. These conditions could have significantly increased soil temperatures providing conditions for slow mineralization of organic carbon deposits by microbes in low oxygen conditions, thus reducing the size of the organic carbon pool (Schuur et al. 2015). In total, the carbon pool over land is estimated to be between 1300-1600 Pg, of which about 400 Pg are below the depth of 3 m, while there is an additional quantity over continental shelf of the Arctic Ocean (Schuur et al. 2015). In the Arctic Ocean there are between 2 and 1400 Pg of permafrost carbon (James et al. 2016). In addition, the Arctic Ocean contains between 100 and 9000 Pg of carbon in the form of methane hydrates (James et al. 2016).

Figure 3. Carbon content (kg C/m²) in the near surface layer of permafrost within the depth of 3 meters based on data from Hugelius et al (2014).



When permafrost thaws, organic carbon becomes exposed to the microbial activity. As a consequence the ground layer emits greenhouse gasses into the atmosphere. At the large spatial scale the decomposability of carbon in permafrost layers mainly depends on the carbon to nitrogen ratio of the organic matter (Schuur et al. 2015). Microbes process organic carbon for energy and grow by using nitrogen released during the decomposition process. According to this ratio soils can be roughly divided into organic with carbon to nitrogen ratio above 20% and mineral with lower ratios (Schuur et al. 2015). It is experimentally found that at soil temperatures of 5 °C the decomposition rate of carbon in organic soils is 17%-34%, while in mineral soils it is 6%-13% per decade (Schuur et al. 2015). Oxygen concentration in the soil saturated by carbon is another factor

controlling the decomposition. Generally, emissions from thawed dryer soil with aerobic conditions contain less methane and more carbon dioxide than emissions from wetter soil with anaerobic conditions (Schuur et al. 2015). Although methane is a much stronger greenhouse gas than carbon dioxide, its global warming impact is distributed over the shorter time period. The atmospheric lifetime of carbon dioxide is also much more complex and may depend on many factors (Archer et al. 2009). On the decadal scale emissions from wet anaerobic soils would more strongly impact global warming by emitting more methane, but over hundred years long time span emissions from dryer soils could become more important for global warming due to longer impact of carbon dioxide (Schuur et al. 2015). These estimates on emission rates from different soil types are mainly based on controlled laboratory experiments and are still not fully established from field campaigns. There are also other impacts of the permafrost thawing on global warming, like heat production from microbial metabolism of organic material (AMAP 2015) and increase of nitrous oxide emissions (Voigt et al. 2017). These additional impacts will not be evaluated in the study.

Permafrost geographical area is characterized by a low density of population. Depending on the geographical definition of the Arctic, it is estimated that between 4 and 10 million people live over Arctic permafrost areas (Blunden and Arndt 2017). The majority of population is in the Russian Federation. Although the Arctic is abundant with natural resources, harsh climate conditions strongly limit human activities. Oil and gas on land is mainly located in Western Siberia. Strong dynamical evolution of permafrost due to thawing and freezing may impact basement of constructions. Many constructions, including infrastructure, residential buildings, pipelines, roads, railroads and runways, suffer damages due to the seasonal and inter-annual variability of soil conditions (Blunden and Arndt 2017).

Global warming is particularly enhanced in the Arctic (e.g. Pithan and Mauritsen 2014). Future rise of temperatures in the Arctic may strongly impact the permafrost by thawing ice at the bottom of the active layer (Biskaborn et al. 2019, Nitze et al. 2018). This process may strongly impact human activities depending on the permafrost, ecology over the permafrost area and expose large quantities of organic carbon to microbial activity producing additional emissions of greenhouse gasses into the atmosphere.

European Union policy for the Arctic, represented in the Joint Communication by the European Commission and High Representative of the Union for Foreign Affairs and Security Policy to the European Parliament and Council “An integrated European Union policy for the Arctic”¹, addresses consequences of accelerated thawing of permafrost by stating: “Greenhouse gases are escaping the permafrost and entering the atmosphere at an increasing rate. The thawing permafrost has the potential to release carbon dioxide and methane - equivalent to several times today’s annual greenhouse gas emissions from man-made sources such as fossil fuel use. This could change the Arctic as well as the global climate.”

The European Union policy for the Arctic is implemented by the Northern Dimension policy² promoting dialogue and cooperation in the Arctic and strengthening the stability and sustainable economic development. The European Union supports the scientific research in the Arctic by financing a number of research projects. In particular, the ongoing Nunataryuk project³ studies the processes involving permafrost thawing, the risks for the local population and impacts on the global society. The European Commission participates in the Working Groups of the Arctic Council, for example the DG-JRC contributes to the scientific activities of the Arctic Monitoring and Assessment Programme (AMAP) to estimate the impacts of short-lived climate pollutants in the Arctic and possible mitigation measures.

The Paris Agreement⁴ aiming at limiting the global atmospheric temperature increase at 2 °C at the end of the century aims to: “reach global peaking of greenhouse gas emissions as soon as possible, ..., and to undertake rapid reductions thereafter in accordance with best available science, so as to achieve a balance between anthropogenic emissions by sources and removals by sinks of greenhouse gases in the second half of this century.”

The large possible release of CH₄ and CO₂ from the thawing permafrost may strongly impact the global temperature change at the end of this and in the next century. It is, therefore, important to estimate already now the future emissions from the permafrost in order to adjust anthropogenic emissions limiting global warming at the end of the century.

By evaluating existing data sets and reviewing existing literature, this report will present estimates the carbon release from the Arctic into the atmosphere due to thawing permafrost in the warmer future climate. In

¹ http://eeas.europa.eu/archives/docs/arctic_region/docs/160427_joint-communication-an-integrated-european-union-policy-for-the-arctic_en.pdf

² https://eeas.europa.eu/diplomatic-network/northern-dimension_en

³ <https://www.nunataryuk.org>

⁴ <https://unfccc.int/sites/default/files/resource/docs/2015/cop21/eng/10a01.pdf>

particular, it will make estimates for current and future natural emissions of CH₄ in the Arctic and compare them with CO₂ emissions in the Arctic and globally. It will also address the impact of thawing permafrost on constructions in the Arctic, by evaluating the influence of thawing on energy exploration, production and transport. Some emerging aspects of the permafrost thawing, like the risk of outbreaks of infective diseases (e.g. Revich et al. 2011), release of long-term accumulated pollutants (e.g. Schuster et al. 2018) or global economic aspects (e.g. Hope Schaefer 2016), will not be considered in the study and may be included in future reports estimating impacts of permafrost thawing.

2 Current and future temperature increase in the Arctic

2.1 Current near-surface temperature trends

Global warming impacts temperatures in the Northern hemisphere in a non-uniform manner. During the last 35 years, since 1980, satellites provide continuous observations of the Earth surface. In this period, it is observed that, although there is a general warming trend, some areas and regions experience strong increase of temperatures, while in others changes appear to be negligible or there is even a cooling trend.

Box 2. Estimates of temperature trends

One way to estimate ongoing changes in the atmosphere, surface ocean and land is to use atmospheric reanalysis produced during the period with satellite observations from 1980 till today. In this period satellites mainly observe change of temperatures on the Earth surface, change of sea-ice and snow cover, intensity and direction of winds over the ocean, and atmospheric irradiances that provide information on mean temperature of the atmospheric column. Most of land and ocean areas in the Northern Hemisphere are also covered by in situ observations at the surface of a large number of parameters, temperature and wind observations made by commercial airplanes, while many vertical soundings observe temperature, humidity and winds. In situ observations are, however mainly located in densely populated areas. Over the northern latitudes and especially in the Arctic there are much less in situ observations than over the lower latitudes.

In Fig. 4 two independent reanalysis products, ERA-INTERIM and NCEP, show that in winter the strongest warming is over the Arctic Ocean. Over the Middle East, South-East Asia, the western Pacific Ocean, Central America and the tropical Atlantic Ocean warming is also strong and consistent in both analysis. In lower latitudes there is cooling trend over the eastern Pacific Ocean. In both ERA-INTERIM and NCEP reanalysis the strongest warming is in the Atlantic sector of the Arctic Ocean indicating reduction of sea-ice cover over the Barents Sea and between Canada and Greenland. On the other hand, the warming in Alaska and land areas of Northern Canada is generally weaker and inconsistent in the two reanalyses. Furthermore, both ERA-INTERIM and NCEP indicate a strong cooling trend in Siberia. The only land area in the Arctic with a clear warming trend in winter is North-Eastern Canada close to the strong sea-ice melting area between Canada and Greenland. Over other land areas near-surface temperatures in winter do not change systematically or even have a negative trend.

In both ERA-INTERIM and NCEP reanalyses in summer trends over lower latitudes are similar to those in winter (Fig. 5). Warming trends are present over the Middle East, South-East Asia, Central America, the western Pacific Ocean and tropical Atlantic. The cooling trend over the eastern Pacific Ocean is weaker than in winter. In higher latitudes, there is approximately uniform warming over land and ocean. Warming is more intense in Eastern and Central Siberia, Alaska and north-eastern Canada.

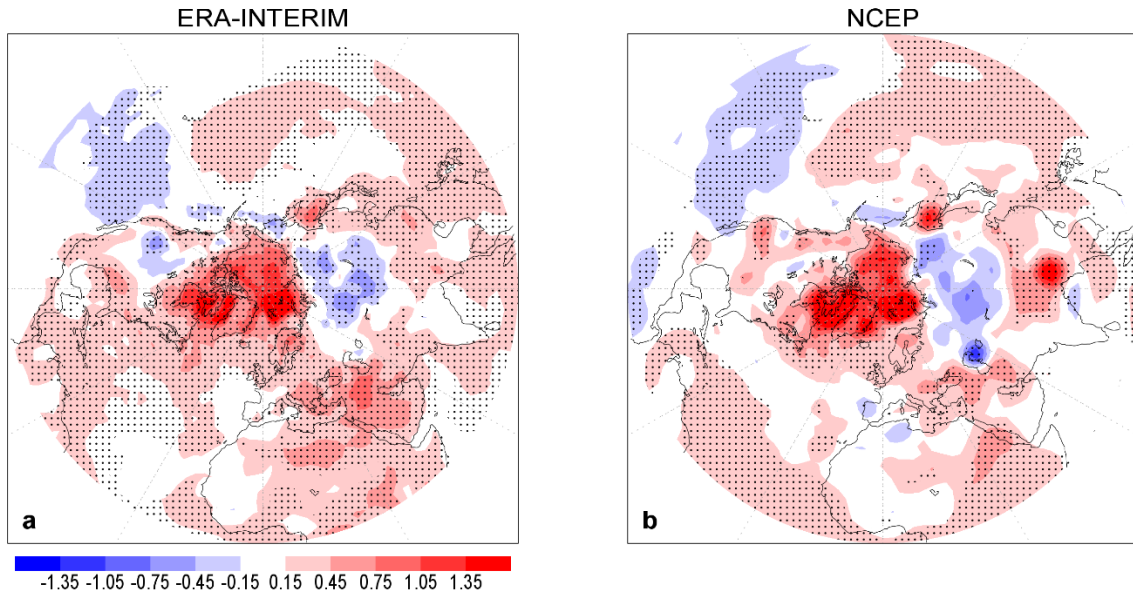
Mostly non-existing warming trends in winter and strong warming trends in summer over the land in the Arctic indicate that the seasonal change of temperatures over the permafrost becomes larger. Furthermore, warmer summer temperatures may thaw deeper layers of ground. As a consequence, we may expect a trend of larger seasonal temperature evolution in the permafrost active layer. The minimum active layer temperatures should not change significantly, while summer temperatures should become higher and the active layer should become deeper.

Box 3. Atmospheric reanalysis

Atmospheric reanalysis combine information from short term forecasts by the global atmospheric model with all satellite and in situ observations in a dynamically and statistically optimal way that is as much as possible consistent throughout the analysed time period. In an implicit way, this procedure combines the best theoretical knowledge with historical information from different instruments, parameters and makes the best possible estimates in areas lacking dense observational networks. The uncertainty of reanalysis strongly depends on the availability of observations. This reduces their accuracy over the Arctic Ocean where temperature observations are sparser than over populated regions of the Northern Hemisphere. On the other hand, over the land even in the Arctic observational network is sufficiently dense to resolve large-scale spatial distribution of near-surface temperatures. At the seasonal scale satellite observations of sea-ice coverage and sea surface temperature should be sufficiently accurate for the evaluation of trends. In this report estimates of trends of physical parameters over the land and ocean will be made by using ERA-INTERIM reanalysis made by the European Centre for the Medium Range Weather Forecasting (ECMWF) (Dee et al. 2011) and National Centre for Environmental prediction (NCEP) reanalysis (Kalnay et al. 1996). The differences between estimates by ERA-INTERIM and NCEP will indicate uncertainties. Both reanalysis cover period after 1980 when satellite observations provide additional observations over the Arctic.

Although their relative importance has not been established yet, several local processes may accelerate the Arctic warming. In summer, due to global warming larger areas of the ocean and land become free of ice and snow. The change of albedo from almost fully reflecting white surface to the almost fully absorbing water or land surface accelerates the accumulation of heat in the ocean and ground (Serreze and Francis, 2006; Kashiwase et al., 2017). In a feedback process heat accumulated in the ocean and ground accelerates warming in the surrounding regions.

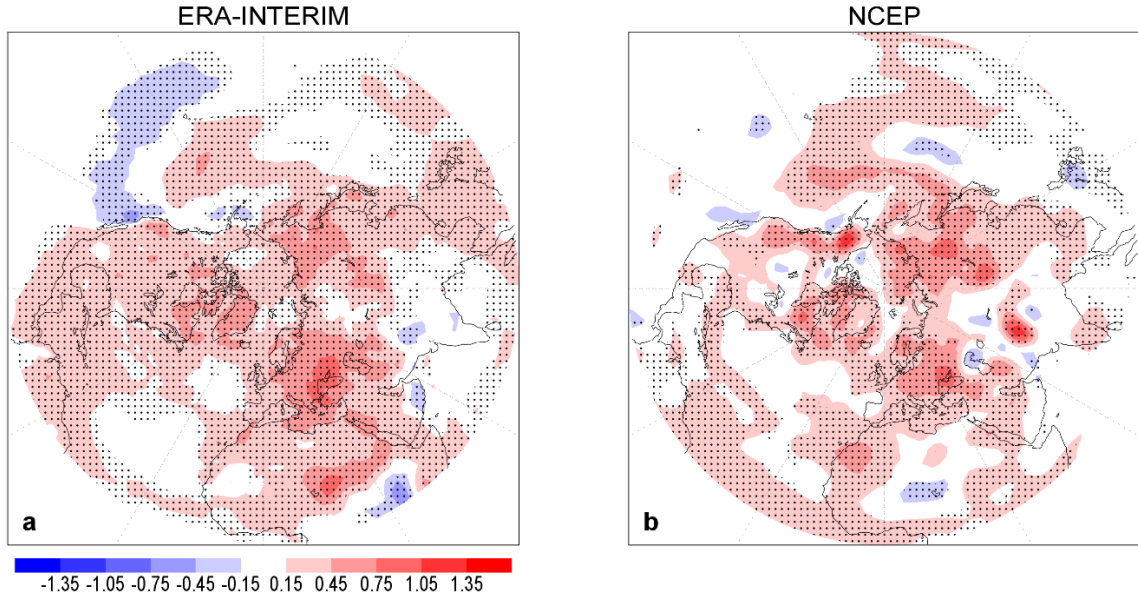
Figure 4. Linear trend of near-surface temperature in winter (December–January–February) ($^{\circ}\text{C}/\text{decade}$) between 1980 and 2015. a) ERA-INTERIM reanalysis and b) NCEP reanalysis.



The Arctic may also warm more rapidly than the global average due to the deposition of black carbon on the sea-ice (Clarke et al., 1985). Even small concentrations of deposited black carbon may modify the albedo and accelerate the sea-ice melting. Another important process for the amplification of arctic warming is the global temperature feedback (Pithan and Mauritsen, 2014). Consistently with the Plank law, the same additional flux of heat produces larger temperature increase when the background atmospheric temperature is colder due to the lower infrared radiation back to the space. This process alone is sufficient to significantly increase the warming rate in the Arctic with respect to the tropics. Another process associated with the global temperature feedback is that in the tropics additional heat at the surface is redistributed by convective clouds into the upper troposphere, while in the higher latitudes, due to the stronger vertical stability, it remains confined to the surface. Oscillations over the tropical Pacific Ocean (Ding et al., 2014) or variability of the middle latitude sea surface temperatures (Peings and Magnusdottir, 2014; Perlitz et al., 2015) may initiate long-standing

planetary waves that increase the advection of northward transport from the middle latitudes into the Arctic and regionally enhance the warming. Warming of the Atlantic Ocean can create positive anomalies in the oceanographic heat transport into the Arctic (Årthun et al., 2012). As a consequence, sea-ice melting in the Arctic Ocean may be accelerated starting the feedback process that may influence temperature trends over the surrounding land.

Figure 5. Linear trend of near-surface temperature in summer (June–July–August) ($^{\circ}\text{C}/\text{decade}$) between 1980 and 2015.
a) ERA-INTERIM reanalysis and b) NCEP reanalysis.



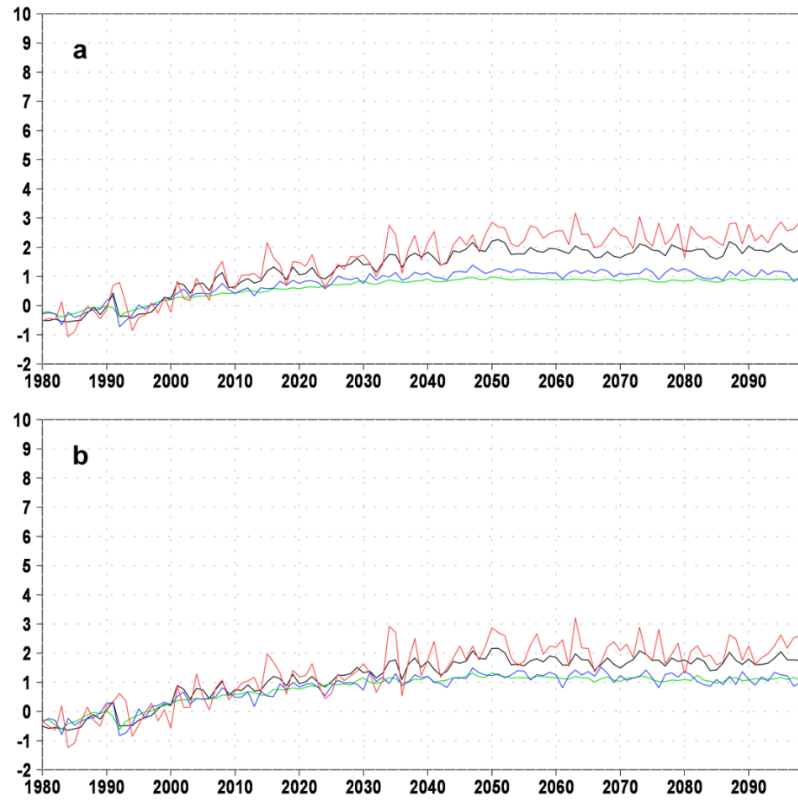
Trends shown in Figs. 4 and 5 are consistent with trends estimated by objective analysis of near surface temperatures in which estimates in areas not covered by observations are obtained by interpolating in a statistically optimal way from points with observations (e.g. AMAP 2015). The change between 1980 and 2015 of annually averaged temperatures over the region north of 60°N is 1.9°C in the ERA-INTERIM reanalysis (Fig. 12, in the Appendix) and 1.2°C in the NCEP reanalysis (Fig. 13, in the Appendix). The change between 1980 and 2012 of annually averaged temperatures over the same region is estimated by three objective analysis to be 1.6°C (AMAP 2015) that is similar to the change estimated by ERA-INTERIM and NCEP estimates.

2.2 Future near-surface temperature trends

The evaluation of future near-surface temperature trends in the Arctic in relation to the global warming may be made from Coupled model intercomparison project version 5 (CMIP5, Taylor et al., 2012) numerical simulations (Box 4). In particular, the evaluation of temperature will be made by using the CESM model with the horizontal resolution of approximately 1° latitude $\times 1^{\circ}$ longitude. The numerical model simulation has 6 ensemble members initiated with slightly different initial conditions. This particular model is selected instead of the whole ensemble, because it has the largest number of layers in the soil and ensemble members. It also has a high horizontal resolution when compared to other CMIP5 models. Two Representative Concentration Pathways (RCP) scenarios will be used. The first is RCP 2.6 that, with respect to the reference period between 1986 and 2005, at the end of the 21st century predicts 1°C higher global temperatures averaged over all CMIP5 model simulations. The second is RCP 8.5 that at the end of the 21st century predicts 3.7°C higher global temperatures.

Fig. 6 shows that in RCP2.6 scenario at the end of the 21st century yearly averaged temperatures rise to two times higher values over the Arctic than globally. In the Arctic, there is also a larger interannual variability and variability between ensemble members as indicated by the larger spread of estimates. When only land points are included in the calculation of temperature change there is a similar increase of yearly averaged temperatures over the Arctic with respect to global temperature rise. The amplification of global warming in the arctic is seasonally dependent. In winter there is a strong amplification and the large interannual variability. On the other hand, in summer the amplification is almost nonexistent. In particular, in summer land points become warmer at the same rate as the globally averaged values over land.

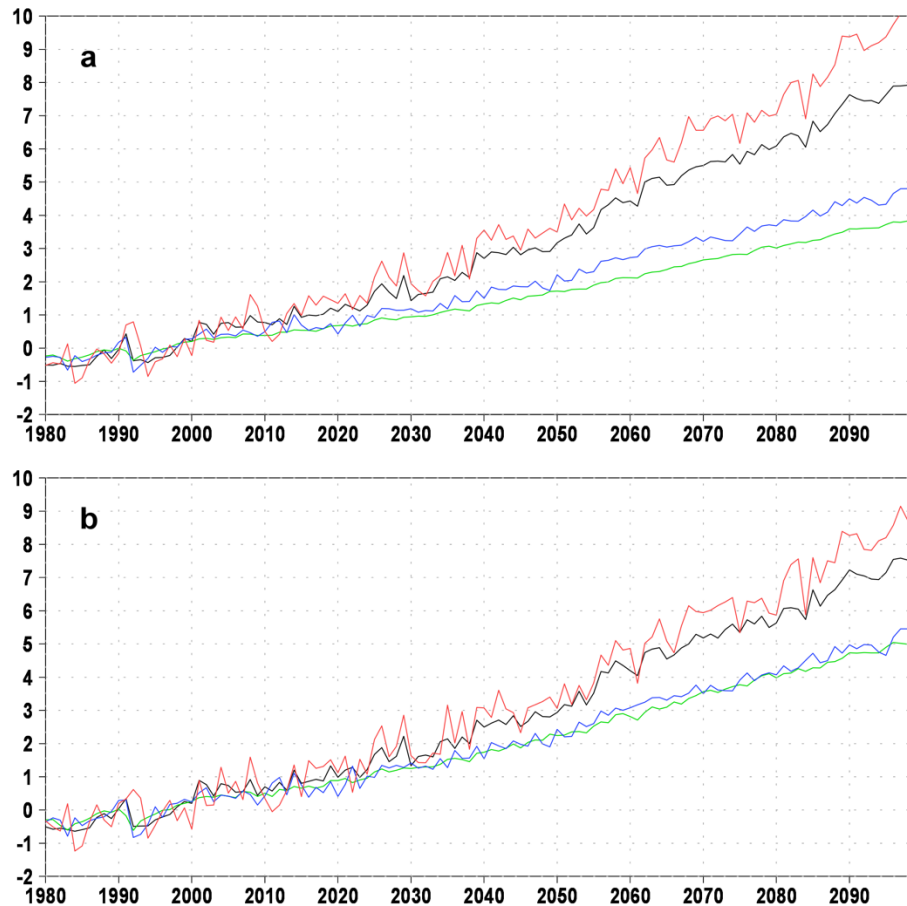
Figure 6. CESM ensemble mean of near-surface temperature change in the RCP2.6 scenario: yearly averaged global temperature (green), yearly averaged temperature north of 60°N (black), winter (January–February–March) averaged temperature north of 60°N (red) and summer (June–July–August) averaged temperature north of 60°N (blue). Panel a shows averages over land and ocean, and panel b averages only over land.



In RCP 8.5 scenario the ensemble mean reaches globally averaged temperatures in 2100 that are 3.8 °C warmer than the 1986–2005 mean values (Fig. 7). There is a strong warming amplification in the Arctic reaching temperatures that are 7.5 °C warmer than the 1986–2005 mean. Like in the RCP 2.6 scenario the amplification is strongly pronounced in winter with values that are 10 °C higher at the end of the 21st century. In winter, there is also the largest interannual variability. In summer the Arctic amplification is much smaller and there is a smaller interannual variability. Over land the amplification is slightly weaker in winter. Like in the RCP 2.6 scenario, in summer land areas in the Arctic have the same warming rate like global land areas.

CESM estimates in the period forced by historical drivers may be compared to reanalysis estimates presented in the previous section. In the Appendix, Fig. 14 shows that, in agreement with reanalyses shown in Figs. 12 and 13, in the period 1980–2015 CESM simulations show globally increasing temperatures and Arctic amplification of global warming.

Figure 7. Same as Fig. 6, but for RCP 8.5 scenario.



Over land areas the Arctic warming in CESM simulation is enhanced in winter and practically equal to the global land warming in summer. This differs from the reanalyses estimates. In the reanalyses the warming is significant in summer, while in winter there is no tendency. Also, in the reanalyses only in summer there is the enhancement of Arctic warming.

The disagreement in estimating the seasonal cycle of Arctic enhancement of global warming may be important for estimating the warming of permafrost. In CESM the yearly averaged Arctic amplification of warming of soil in deeper layer appears to be due to enhanced Arctic warming in winter, because higher winter temperatures contribute to summer warming by producing spring temperatures closer to the freezing point and facilitating the penetration of heat into the soil in summer. On the other hand reanalysis indicate that currently the warming of deeper soils is mainly due to higher temperatures in summer that may produce deeper active layers.

The fact that CESM simulation in CMIP5 agrees with the reanalysis in estimating the Arctic warming about twice as large as the global average should be carefully interpreted when estimating the impact on the soil temperature. Higher summer trend of near-surface temperature in the reanalyses indicates that near-surface soil temperatures are also higher than in the CESM simulation providing conditions for the more intense microbial activity producing carbon fluxes into the atmosphere.

Box 4. CMIP5 and RCPs

The fifth phase of the Coupled Model Intercomparison Project (CMIP5) provided a framework for coordinated climate change experiments for the fifth Assessment Report (AR5) of the Intergovernmental Panel on Climate Change (IPCC). The multi-model experiments provided the opportunity to assess the mechanisms responsible for model differences in poorly understood feedbacks associated with the carbon cycle and with clouds, to examine climate predictability and to explore the ability of models to predict climate on decadal time scales, and, more generally, to determine why similarly forced models produce a range of responses. More than 20 climate models participated to the CMIP5 experiments and their results are freely available (e.g. http://www.ipcc-data.org/sim/gcm_monthly/AR5/Reference-Archive.html). The CMIP5 experiment design was finalized with the following suites of experiments: Hindcasts (historical) simulations; future "long-term" simulations; "atmosphere-only" (prescribed SST) simulations for especially computationally-demanding models.

The simulations of the climate in the future follow the so-called Representative Concentration Pathways (RCPs), which are not a complete package of socioeconomic, emissions, and climate projections, but consistent sets of projections of only the components of radiative forcing that are meant to serve as input for climate modelling. The RCPs were chosen to represent a span of the radiative forcing and facilitate the mapping of a broad climate space. They therefore do not represent specific futures with respect to climate policy action (or no action) or technological, economic, or political viability of specific future pathways or climates. Four RCPs were developed by four independent modelling groups:

- RCP2.6: very low GHG concentration levels, with a peak radiative forcing (RF) of 3.1 W/m² at mid-century, dropping to 2.6 W/m² by 2100, through a substantial GHG emission reductions over time (van Vuuren et al., 2007).
- RCP4.5: the total RF is stabilized at 4.5 W/m² before 2100 by employment of a range of technologies and strategies for reducing greenhouse gas emissions (Clarke et al. 2007; Wise et al (2009)).
- RCP6.0: the total RF is stabilized at 6.0 W/m² after 2100 without overshoot by employment of a range of technologies and strategies for reducing greenhouse gas emissions (Fujino et al. 2006, Hijioka et al. 2008).
- RCP8.5: increasing greenhouse gas emissions over time representative for scenarios in the literature leading to high greenhouse gas concentration levels (Riahi et al. 2007).

3 Potential for methane and carbon dioxide release from permafrost thawing

Methane emissions from permafrost thawing are especially important due to high warming effect in the atmosphere. On the other hand, large emissions of carbon dioxide may also significantly impact global warming. Although carbon dioxide has a smaller warming effect than methane, it remains for long time in the atmosphere. It is, therefore, important to estimate how much carbon in the permafrost will be available in the future for the microbial degradation and provide emission source for both atmospheric methane and carbon dioxide. The largest microbial activity over the permafrost area is in summer when near-surface temperatures are the highest. Due to global warming near-surface temperatures will rise and the active layer will warm. As a consequence active layer may either become deeper, or its temperatures may rise while its depth may remain invariant.

In the next sections we provide an estimate of the total carbon in soil which may be available in the future for microbial degradation (Section 3.1) with consequent emission of carbon dioxide (Section 3.2). The carbon content that is available for microbial degradation is estimated by combining estimates of soil temperatures by reanalysis (Box 2) and CMIP5 simulations (Box 3) with estimates of total carbon content per square meter over the permafrost area from Hugelius et al. (2014) (Box 1). ERA-INTERIM and NCEP reanalysis are used in the period 1980-2015. CMIP5 ensemble simulations by three models (CESM, IPSL and MPI) are used to estimate change of soil temperature in three RCP scenarios, RCP 2.6, 4.5 and 8.5 (Box 3). The discussion of current and future methane emissions associated to permafrost thawing and boreal wetlands formation, as well as deposits of methane-hydrates in the Arctic Ocean is based on the latest scientific studies (Sections 3.3 and 3.4).

3.1 Present and future carbon availability in unfrozen soils

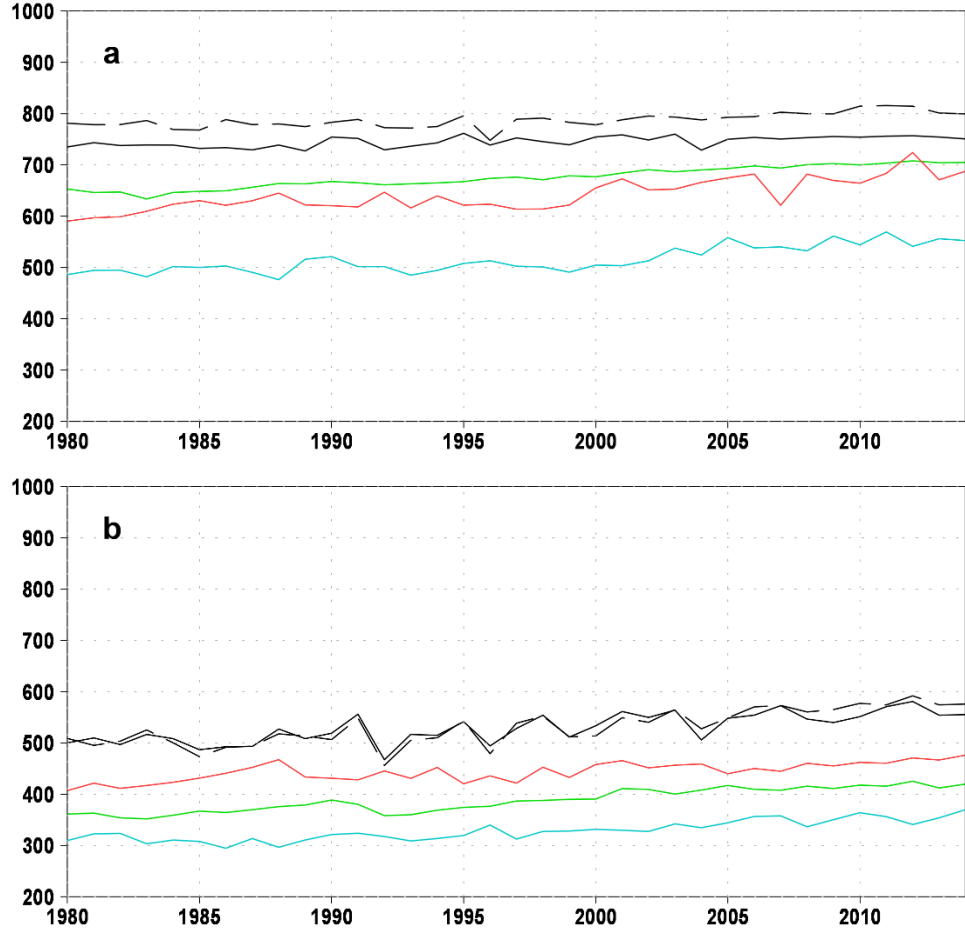
For our estimates we have used monthly mean temperatures in soil layers of the atmospheric reanalysis and CMIP5 climate models. The depth of the active layer is estimated from the freezing level calculated from the linear interpolation of temperatures between the maximum level at which the temperature is above the freezing level during the year and the level below. The carbon content is then calculated by integrating the mass of carbon content estimated by Hugelius et al. (2014) from the lowest freezing level to the surface. The carbon content below the depth of 3 m is not considered in this study.

Fig. 8 shows the estimated change between 1980 and 2015 of carbon content in the active layer with temperatures above 0 °C in summer. ERA-INTERIM and NCEP analysis show that the mean active layer becomes larger due to global warming (Fig. 8a), although the rise of carbon content is small with respect to the mean value. It is also smaller than the average difference between ERA-INTERIM and NCEP reanalysis. The three historical CMIP5 ensemble simulations show lower carbon content estimates in the active layer than reanalysis. They also show the stronger increase of carbon content available for degradation in the last decades.

It is also interesting to evaluate the quantity of carbon in the active layer at higher temperatures than the freezing point. At higher temperatures the microbial activity is stronger (e.g. Schuur et al. 2015). Fig. 8b shows carbon content in the active layer in summer that is at temperatures higher or equal to 5 °C. By using experimental data it is assumed that these temperatures provide environmental conditions for a larger microbial decomposition than temperatures between 0 °C and 5 °C (e.g. Schuur et al. 2015). In ERA-INTERIM and NCEP carbon content at temperatures above 5 °C is about two thirds of the carbon content above the freezing point. Both reanalysis show very similar estimates. The trend in the reanalysis is especially pronounced in the last 20 years. It starts from 500 Pg in 1995 and reaches almost 600 Pg in 2015. Like in the case of temperatures above the freezing point, the three CMIP5 ensemble simulations show lower estimates of carbon at temperatures above 5 °C than the two reanalysis with values that are about two thirds of values estimated in the active layer. On the other hand, trends of CMIP5 simulations are very similar to those estimated by the reanalysis.

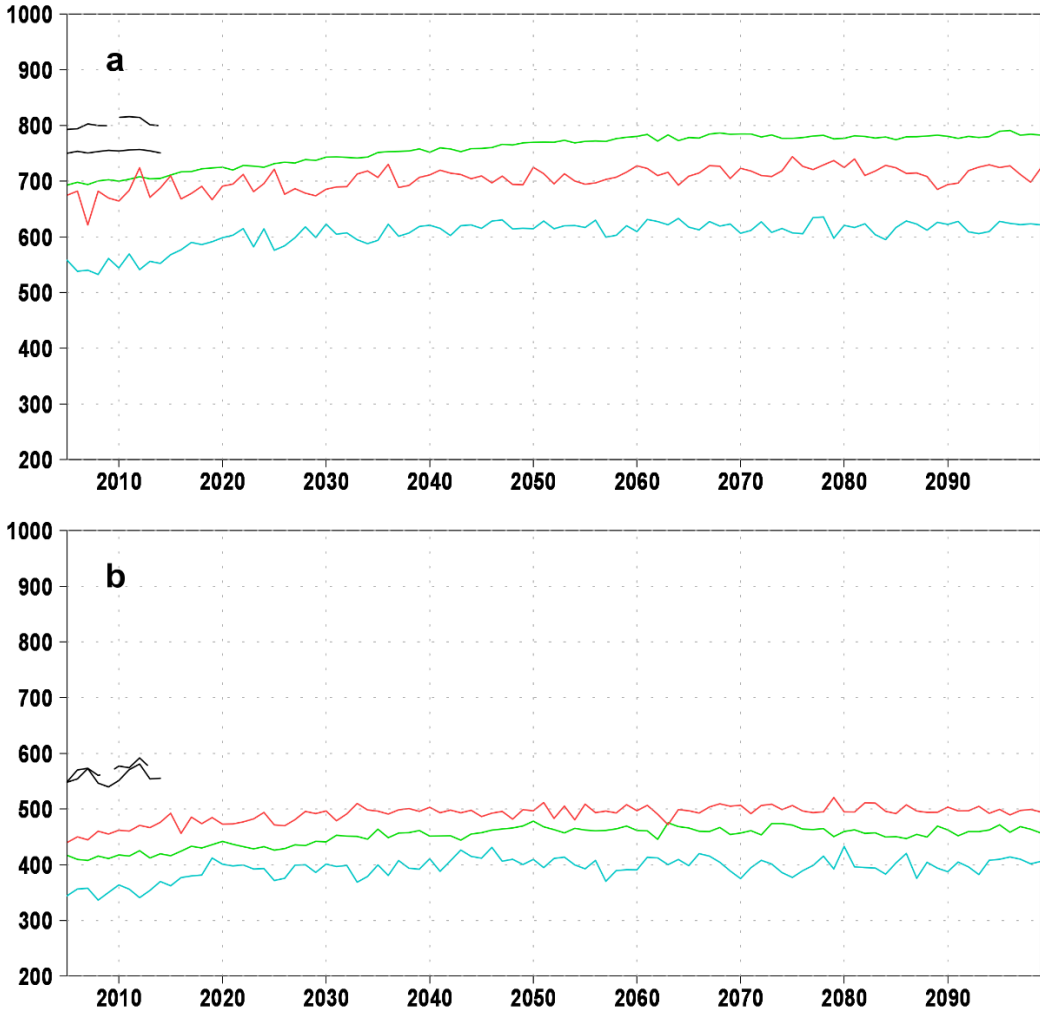
These findings may be compared with other studies involving estimates of the exposed carbon content from CMIP5 simulations made by simplified models similar to the one used in this study (Koven et al. 2013, Burke and Jones 2013). Those studies show a large divergence between different CMIP5 model estimates of carbon content inside the active layer. On the other hand, this study selected CMIP5 models with the largest number of vertical levels and ensemble members and the highest horizontal resolutions. It is assumed that these models may provide the most accurate simulation of soil temperatures. With this selection, the differences between CMIP5 model estimates of carbon content inside the active layer are approximately constant throughout the evaluation period and all models show very similar trends. In the period 1980-2015 trends are further similar to those estimated from the reanalysis.

Figure 8. Estimated carbon content in the permafrost (Pg) in summer (June–July–August) between 1980 and 2015: a) inside the active layer and b) in the soil with temperatures higher than 5 °C. Soil temperatures are estimated by ERA-INTERIM reanalysis (full black), NCEP reanalysis (dashed black), mean of 6 CESM CMIP5 simulations (green), mean of 3 IPSL CMIP5 simulations (red) and mean of 3 MPI CMIP5 simulations (cyan). CMIP5 simulations used historical forcing between 1980 and 2005, and RCP 2.6 forcing after 2005.



While in ERA-INTERIM and NCEP carbon content in the active layer differs by a constant value throughout the period spanning the last decades, above 5 °C the two reanalysis show almost identical estimates. The reason is that reanalysis use climatological temperatures at bottom layers of their land models. These estimates may differ and impact estimates of active layer depths. The isotherm of 5 °C is closer to the surface. It is less influenced by climatological values at the bottom of the land model and more by conditions at the surface. Due to very similar surface forcing in the two reanalysis carbon content estimates above 5 °C are also very similar. In CMIP5 simulations bottom layer temperatures are not constrained by climatology and their trends of carbon content are stronger than in the reanalysis. Due to more similar forcing conditions in CMIP5 simulations and reanalysis, CMIP5 estimates of trends of carbon content at temperatures above 5 °C become very similar to trends in the reanalysis. Similar trends between the CMIP5 simulations and reanalysis indicate that during the last decades CMIP5 simulations correctly depicted the change of carbon content in the active layer and at temperatures above 5 °C. This may give confidence in interpreting future estimates of carbon content under different global warming scenarios.

Figure 9. Estimated carbon content in permafrost (Pg) in summer (June–July–August) between 2006 and 2100: a) inside the active layer and b) in the soil with temperatures higher than 5 °C. Soil temperatures are estimated by ERA-INTERIM reanalysis (full black), NCEP reanalysis (dashed black), mean of 6 CESM CMIP5 simulations (green), mean of 3 IPSL CMIP5 simulations (red) and mean of 3 MPI CMIP5 simulations (cyan). CMIP5 simulations were forced by RCP 2.6 scenario.



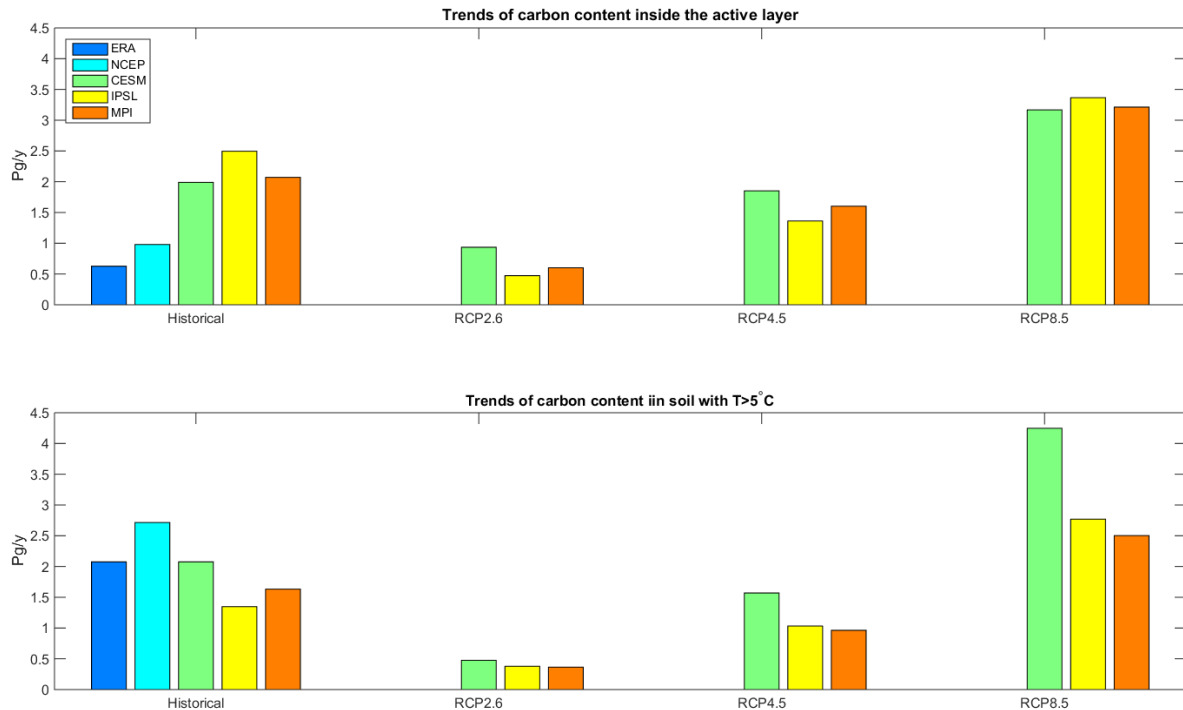
In the 21st century the carbon content in the active layer estimated by CMIP5 simulations changes accordingly to carbon dioxide concentration scenarios. In RCP 2.6, corresponding to global warming of 1 °C in 2100, the total change between the beginning and end of the 21st century is modest and comparable to the total change in last three decades (Fig. 9a). In RCP4.5, which corresponds to global warming of about 2 °C in 2100, the rate of change is stronger and similar to CMIP5 estimates of the current rate (Fig. 15a, Appendix). In RCP8.5, with global warming of about 4 °C in 2100, the rate increases to almost twice the current rate (Fig. 16a, Appendix).

In RCP 2.6 total carbon content above 5 °C isotherm does not change significantly between the beginning and end of the 21st century (Fig. 9b). In RCP 4.5 it continues to rise by the similar rate as in the last decades (Fig. 15b, Appendix). At the end of the century it reaches values that are about 25% higher than current estimate. In RCP 8.5 the rise accelerates reaching values that are almost twice as large as the current estimates (Fig. 16b, Appendix).

The spatial structure of carbon content change in the 21st century in the RCP 2.6 scenario shows that, while in some areas it becomes larger, in other areas it remains unchanged or even diminishes (Fig. 17, Appendix). Different models provide very different spatial distributions. This indicates that differences are mainly due to internal climate variability that is differently simulated in each CMIP5 ensemble, while global warming has a small impact. In the RCP4.5 scenario areas with increasing carbon content dominates in all CMIP5 ensembles, but still the spatial distribution may differ (Fig. 18, Appendix). In this scenario global warming influences total values, but the spatial distribution is still strongly influenced by the internal climate variability. In the RCP 8.5 scenario carbon content increases with a more similar spatial distribution among CMIP5 ensembles. Still there are some significant differences in the distribution with areas that show reductions (Fig. 19, Appendix). Even in

this scenario the internal climate variability may strongly influence the spatial distribution of areas in which carbon content becomes available for the microbial activity in summer.

Figure 10. Linear trends of carbon content (Pg C/y) at temperatures above 0 °C (top) and above 5 °C (bottom) in the historical period (1986–2005) and for the three RCP scenarios in the 21st century (2006–2100). All trends are statistically significant at 0.05 value. Trends do not contain estimates of microbial activity.



Figs. 17–19 in the Appendix show that often the reduction of carbon content in the active layer is associated with the increase of carbon content at temperatures above 5 °C. The reason for this relationship may be that, due to soil and vegetation properties, the increase of near-surface temperatures by global warming may increase energy in the soil in two distinct processes. In one process warming of the soil penetrates deeper. The additional energy is used for thawing permafrost, while due to the diffusion of colder temperatures from lower layers, the 5 °C isotherm may move upwards. On the other hand, if the additional energy due to warming does not penetrate deep and does not thaw additional layers at the bottom, it increases temperatures in the active layer and lowers the 5 °C isotherm. In the second process the unchanged or even shallower active layer depth may result in larger microbial activity and carbon emissions from the ground due to higher temperatures close to the surface.

Table 1. Difference between mean carbon content (Pg) estimated by CMIP5 simulations in periods 2006–2100 and 1986–2005. Differences are made for carbon content at temperatures above 0 °C and 5 °C. Values are given for each CMIP5 ensemble and for the average among all three ensembles.

	Carbon content above 0°C				Carbon content above 5°C			
	CESM	IPSL	MPI	Mean	CESM	IPSL	MPI	Mean
RCP 2.6	64	29	47	47	34	51	49	45
RCP 4.5	94	62	78	78	67	73	69	70
RCP 8.5	134	120	132	129	142	126	112	127

Trends of carbon content available for degradation by microbes are summarized in Fig. 10. As discussed in previous paragraphs, during the last decades the reanalyses show a smaller positive trend of carbon continent in the active layer than simulations, probably due to fixed climatological temperatures at the bottom of the land model. Trends of carbon content above the 5 °C isotherm are similar in reanalysis and the CMIP5 simulations indicating that CMIP5 simulations correctly simulate the warming speed at the surface. With respect to the last three decades, in the 21st century RCP 2.6 and 4.5 scenarios reduce trends of carbon content available for microbial activity, while the trends are increased in the RCP 8.5 scenario. The mean additional carbon content available for degradation by microbes in the 21st century is listed for each CMIP5 ensemble in Table 1.

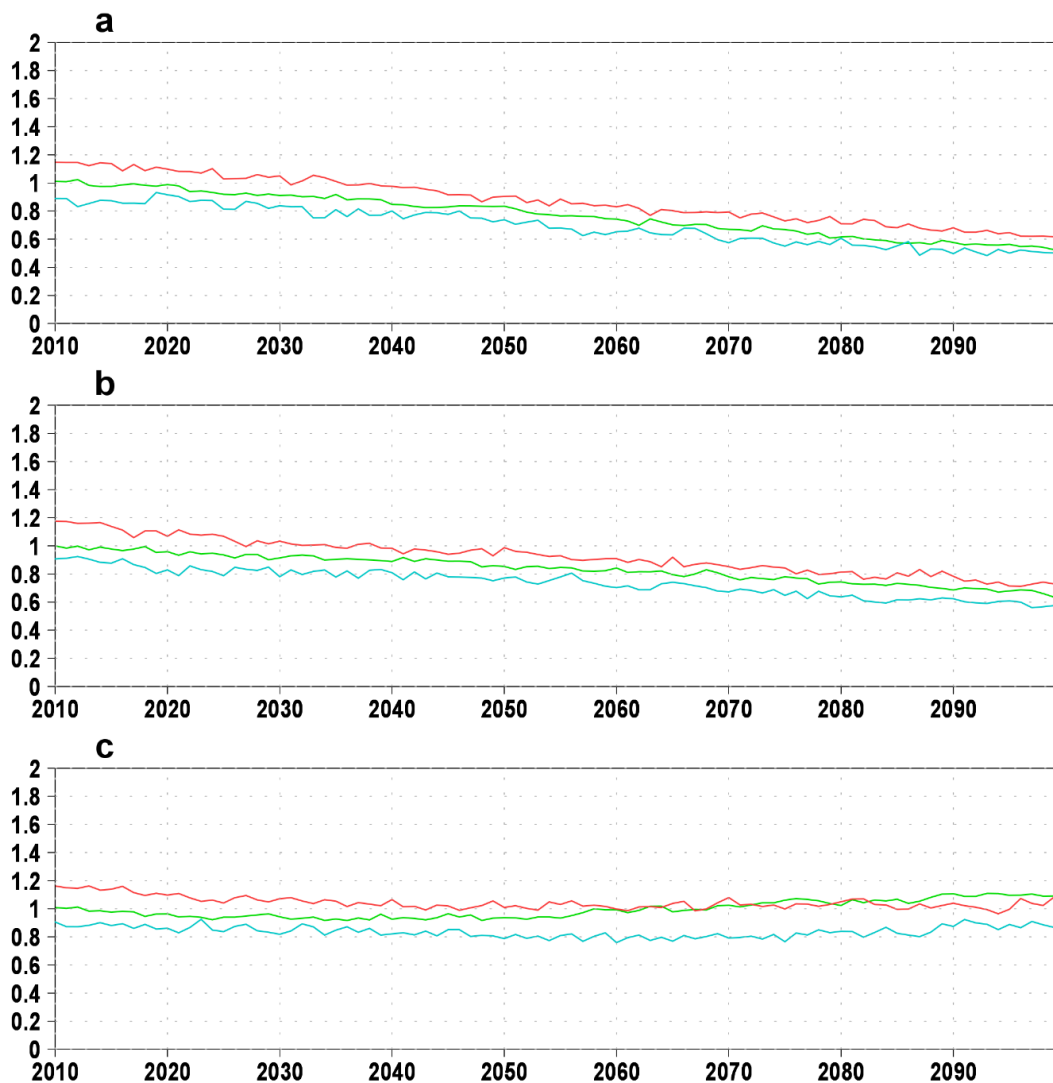
3.2 Carbon dioxide emissions from microbial degradation

By combining carbon content estimates at temperatures above 5 °C with estimates on microbial degradation rate at these temperatures obtained in laboratory experiments (Schuur et al. 2015) it may be possible to estimate carbon emissions into the atmosphere. It is assumed that all emissions are from the dry soil and contribute to the increase of atmospheric carbon dioxide, while methane fluxes are mostly from wetlands requiring only a small fraction of available carbon content. Assuming that the soil is mainly mineral and dry about 1% of soil exposed to microbial degradation at temperatures above 5 °C could be emitted into the atmosphere each year (Schuur et al. 2015). The amount of carbon emissions into the atmosphere each year will, therefore, depend on soil temperature in that year and the rate of depletion of carbon stored in the soil in previous years. A model based on these assumptions may estimate the total emission of carbon in the 21st century.

The model is integrated from 2000 with the initial carbon content estimate from Hugelius et al (2014). Each year 1% of carbon content at temperatures above 5 °C is added to atmospheric emissions and carbon content is reduced by the same amount. Model estimates of carbon emitted into the atmosphere in different RCP scenarios are shown in Fig. 11.

In the RCP 2.6 scenario emissions start to diminish already before 2030. The temperature rise in this scenario is slow and after 2020 every year less carbon is emitted into the atmosphere. In this scenario, global temperatures become lower after 2040. This further reduces the rate of emissions reaching about one half of initial values in 2100. In the 21st century emissions are reduced also in the RCP 4.5 scenario. In 2010 in the RCP4.5 scenario emissions are higher than in the RCP 2.6 scenario. Although in the RCP 4.5 scenario global temperatures do not diminish emissions are reduced due to the depletion of carbon content in the soil by the microbial activity. By the end of the 21st century emissions are lowered by about 25%. Throughout the 21st century emissions in the RCP 8.5 scenario are similar, indicating that the increase of global temperatures producing conditions for the larger microbial activity is mostly compensated by the microbial uptake and reduction of carbon content in the previous years.

Figure 11. Emissions into atmosphere of carbon present in the permafrost (Pg C/y): a) RCP 2.6, b) RCP 4.5 and c) RCP 8.5. Ensemble means are represented by green (CESM), red (IPSL) and cyan (MPI) lines.



Emissions from the existing permafrost carbon in the 21st century are 80 Pg C in RCP2.6, 85 Pg C in RCP 4.5 and 97 Pg C in RCP 8.5. The estimate of 97 Pg C in RCP 8.5 is in a very good agreement with the mean estimate from 8 studies of 92 Pg C (Schuur et al. 2015). It is interesting that, although emissions diminish in RCP 2.6 and 4.5 scenarios, cumulative values are only 20% and 15% lower than in the RCP 8.5 estimate. Estimated yearly emissions averaged over the 21st century in all scenarios are approximately 10% of current global anthropogenic emissions.

The microbial degradation rate may vary around the 1% average between 0.5 and 1.5% within the 0.95 confidence interval (Schuur et al. 2015). The sensitivity of emission estimates on 0.5 and 1.5% degradation rates is shown in Figs. 20-21 (Appendix). In the case of 0.5% degradation rate carbon emissions are significantly lower and in the case of 1.5% rate they are significantly higher than with the 1% rate. In all cases emissions in different RCP scenarios are similar in the first half of the 21st century, while at the end of the century RCP 8.5 scenario is characterized by significantly higher emissions.

When calculating the total carbon over the permafrost area it is also necessary to estimate the increase of carbon content in the soil due to the stronger growth of plants and carbon content in new plants over the warmer soil (Koven et al. 2011, Schaphoff et al. 2013). This process may be more rapid than the depletion of the old carbon in the soil. When taking into account the vegetation development, during most of the 21st century the permafrost area may become a sink of atmospheric carbon. On the long term, towards the end of the 21st century, the sink due to the vegetation impact on carbon content stabilizes and the permafrost zone should become an atmospheric source of carbon (Koven et al. 2011, Schaphoff et al. 2013). By including the vegetation development, it may be estimated that in 2100 in RCP 2.6 there will be a small net increase of soil carbon

content with respect to current values, while in RCP 4.5 carbon content will be slightly decreased and in RCP 8.5 it will decrease by 12-24 Pg C (Schaphoff et al. 2013).

Several recent studies demonstrate that, as models are based on a number of assumptions and poorly resolved parametrizations, there is a limited ability to numerically simulate future vegetation development over the permafrost. In particular, models have difficulties in simulating disturbances in the vegetation development or are unrealistically sensitive to changing climate conditions. There are still very few observations monitoring vegetation changes (Zona 2016) that may support model development. Abbott et al. (2016) find that the major limitations of numerical models are inadequate simulation of river and coastal hydrology and impacts of fires. Based on the opinion of 98 experts, Abbott et al. (2016) estimate that by 2100 permafrost will become atmospheric carbon source independently of the anthropogenic emission scenarios, but the reduction of global warming will also reduce the carbon source from the permafrost. McGuire et al. (2016) find a large variability between estimates by 15 models of the loss of soil carbon between 1960 and 2009 and recommend methodologies for benchmarking models. Natali et al. (2017) experimentally show that a large fraction of carbon production over thawed permafrost is lost by winter respiration and estimate that this process may more than double overall carbon losses from tundra.

While global warming will expose the carbon content stored in the permafrost at the rate which primarily depends on the rate of temperature rise in the Arctic, the amount of compensation by the newly developed vegetation is more difficult to predict. The compensation will strongly depend on environmental processes and disturbances that are very uncertain and difficult to simulate. Most of the studies agree that at the end of the 21st century permafrost will become the source of atmospheric carbon, while the rate of carbon emissions will depend on the global warming rate.

3.3 Methane emissions from boreal wetlands

It is estimated from ice cores that in 1750 atmospheric methane concentration was 720 ppb (Ciais et al. 2013). Since then the concentration rose to more than 1850 ppb at the end of 2017⁵. It is believed that the increase of concentrations in the last 250 years is mainly due to increased anthropogenic emissions (Kirschke et al. 2013). In the last three decades from 1980 to 2015 global atmospheric concentrations of methane showed an increase at the rate of about 7 ppb/y. The rate of 12 ppb/y between 1980 and 1990 decreased to zero between 2000 and 2007 when there was a balance between sources and sinks, and since then methane in the atmosphere has risen at the rate of 5 to 12.5 ppb/y. The main reason for the slowdown of the increasing rate after 1990 and the balance between sinks and sources may be due to the collapse of Soviet Union, while the further decrease between 2000 and 2007 may be due to the strong El Niño in 1998 (Bousquet et al. 2006). Bergamaschi et al. (2013) showed that the recent increase of methane concentrations, following the steady period between 2000 and 2007, was mainly due to sources located in the tropics and mid latitudes. The main driver for increasing emissions was human activity. There was a large inter-annual variability in estimated emissions. In particular, the large variability was obtained for wetland and biomass burning emissions. This study did not show a significant increase of methane emissions from the Arctic. Estimates of emissions in the Arctic are, however, not constrained as much as the estimates in the tropics and mid latitudes. This is due to a poor coverage of the Arctic by in situ network and satellite observations. Furthermore, due to the reduced vertical mixing in the Arctic in situ observations may be representative only for small areas surrounding stations. On the other hand, in 2007 Bergamaschi et al. (2013) found estimates of increased methane emissions from Eastern Siberia. This estimate was consistent with proposed impact due to the increase of near-surface temperatures in Eastern Siberia in 2007 (Dlugokencky et al., 2009). It should be noted that this single-year anomaly in 2007 does not demonstrate the trend in increased methane emissions from the Arctic.

A number of models have been applied to estimate the release of methane from the permafrost. Their complexity ranges from simple empirical formulations to complex ecosystem process models. Statistical models may be formed by regressing methane emissions to environmental parameters (e.g. Moore and Roulet 1993). Daily fluxes may be also estimated from freshwater chemistry, temperature and respiration (e.g. Potter and Klooster 1997). A more sophisticated approach is to include the vertical distribution and types of fluxes (e.g. Cao et al. 1996). The most complex models also include microbial dynamics, water chemistry and soil variability (e.g. Grant 1998).

Mean model estimates of methane emissions from wetland permafrost are estimated to be 37 Tg CH₄/y (Zhang et al. 2013, AMAP 2015), while at the end of the 21st century the flux rises by 30% with respect to the end of the 20th century. This estimate is somewhat higher than the current estimate by inverse modelling of 15 Tg

⁵ Dlugokencky, 2018, https://www.esrl.noaa.gov/gmd/ccgg/trends_ch4/

CH_4/y with uncertainties ranging between 11 to 27 Tg CH_4/y (Bergamaschi et al. 2013, Kirschke et al. 2013, Houweling et al. 2014). In a study involving 11 prediction models Poultier et al. (2017) estimated that due to global warming the boreal wetland contribution to atmospheric methane fluxes increased by 1.2 Tg CH_4/y , compensating a decrease over tropical regions. This study, however, did not separately estimate emissions over the Arctic tundra.

McGuire et al (2012) compared observed emissions, estimates of wetland area in the Arctic and regional process-based model simulations to estimate current tundra emissions of 24 Tg CH_4/y ranging between 10 and 38 Tg CH_4/y . By using the area of wetland tundra McGuire et al. (2012) emission estimate becomes limited between 8 and 15 Tg CH_4/y at the beginning of the 21st century and between 10 and 20 Tg CH_4/y at the end of the century (AMAP 2015).

A major source of uncertainty in modelling emissions from Arctic soils is the wetland area specification. Petrescu et al. (2010) estimated that doubling the wetland area results in four times larger emissions. By taking into account these uncertainties the AMAP assessment report (AMAP 2015) combined estimated area of the wetland tundra, lower and upper estimates of wetland emissions (McGuire et al 2012) and model outputs from Zhang et al (2013). The combined estimate reduced the original model output to about one half of the initial value assuming the large wetland area, and to one quarter assuming the small wetland area. The reduction may be also justified by the fact that Zhang et al. (2013) estimates were higher than estimates by extrapolating in situ measurements of fluxes by McGuire et al (2012) and estimates based on inverse models.

Box 5. Global estimates of methane emissions

Methane emissions may be estimated through different approaches:

- Bottom-up: In the bottom-up approach emissions are first estimated by in situ measurements at representative sites. Then these values are extrapolated over the estimated global extent of individual sources. As such this methodology is not constrained by the atmospheric observations of methane concentration far from sources.
- Top-down (Inverse methods): Typically, starting from initial emission estimates model simulations produce atmospheric methane concentrations that differ from observations. Emissions estimates are then changed in order to bring emission estimates and observations in better agreement by taking into account uncertainties linked to emissions and observations. This may be achieved either by statistical methods based on ensemble model simulations or variationally by using linearized version of the model and backward integration by the transpose operator of the linearized model in order to estimate the sensitivity of observation to changes in emissions. The former approach is named 4D-var indicating its variational approach in the three-dimensional space and temporal variability. In this way, inverse methods represent top-down estimates that are combined with bottom-up information on methane sources available before atmospheric observations. Inverse model estimates contain uncertainties. The most important uncertainty is due to the lack of observational coverage in some areas. Global observing system is based on several tens of land stations mainly concentrated over the most populated areas in the Northern Hemisphere, research ship surveys over the ocean and satellite observations of column averaged concentrations excluding Polar Regions.
- Methane atmospheric concentrations and lifetime: Another method for estimating the total methane emissions uses atmospheric observations of methane concentrations and estimates of atmospheric life time. Hydroxyl determines the loss rate of atmospheric methane and implicitly provides an estimate of methane sources. Top-down estimate in Prather et al. (2012) of 554 (498-600) Tg CH_4/y , is based on combining observations of atmospheric methane and hydroxyl radical.

Main anthropogenic sources of methane in the atmosphere are rice cultivations, domestic animals, landfills and waste, biomass burning and fossil fuels burning. Natural sources of methane are wetlands, lakes and rivers, wild animals, wildfires, termites, geological activity, marine sources and permafrost. Wetlands are the largest natural source of atmospheric methane, globally (Kirschke et al. 2013; Saunois et al., 2016). The estimates of methane emissions are summarized in Tables 1 and 2, for anthropogenic and natural sources, respectively.

The tables collect a large number of studies which applied the two main approaches, the top-down and bottom-up methodologies. Bottom-up method for the period 2000-2009 estimates 678 (483-738) Tg CH₄/y (Kirsche et al. 2013) and 719 (583-861) Tg CH₄/y (Saunois et al., 2016) that are larger than estimates by top-down method of 553 (526-569) Tg CH₄/y (Kirsche et al. 2013) and 552 (535-566) Tg CH₄/y (Saunois et al., 2016). This difference is mainly determined by lower estimates of methane natural emissions in the top-down approach. Natural and anthropogenic sources equally contribute to total methane emissions in the bottom-up method, while top-down estimates partition about 60% of total emissions to anthropogenic sources (Prather et al. 2012). Although the top-down estimate indicates that the bottom-up estimate overestimates emissions, it does not indicate which source may contain the most significant overestimate.

Table 2. Partition of contributions of anthropogenic sources to annual emissions for the period 2000-2009 (Kirschke et al. 2013; Saunois et al., 2016).

	Emission (TgCH ₄ /y)			
	Kirschke et al. 2013		Saunois et al 2016	
Source	Bottom-up	Top-down	Bottom-up	Top-down
Agriculture and waste:	200 [187-224]	209 [180-241]	190 [174-201]	183 [112-241]
<i>Rice production</i>	36 [33-40]		29 [23-35]	
<i>Enteric fermentation & manure</i>	101 [98-105]		103 [95-109]	
<i>Landfills</i>	63 [56-79]		57 [51-61]	
Fossil fuels	96 [85-105]	96 [77-123]	112 [107-126]	101 [77-126]
Biomass burning	35 [32-39]	30 [24-45]	30 [26-34]	35 [16-53]
Total	331 [304-368]	335 [273-409]	338 [329-342]	319 [255-357]

Table 3. Partition of contributions of natural sources to annual emissions for the period 2000-2009 (Kirschke et al. 2013), and 2003-2012 (Saunois et al., 2016).

	Emission (TgCH ₄ /y)			
	Kirschke et al. 2013		Saunois et al 2016	
Source	Bottom-up	Top-down	Bottom-up	Top-down
Wetlands	217 [177-284]	175 [142-208]	185 [153-227]	167 [127-202]
Other natural:	130 [45-232]	43 [37-65]	199 [104-297]	64 [21-132]
<i>Lakes and rivers</i>	40 [8-73]		122 [60-180]	
<i>Wild animals</i>	15 [15-15]		10 [5-15]	
<i>Wildfires</i>	3 [1-5]		3 [1-5]	
<i>Termites</i>	11 [2-22]		9 [3-15]	
<i>Geological</i>	36 [15-57]		40 [30-56]	
<i>Oceanic sources</i>	18 [2-40]		14 [5-25]	
<i>Permafrost</i>	1 [0-1]		1 [0-1]	
Total	347 [238-484]	218 [179-273]	384 [257-524]	231 [194-296]

3.4 Methane emissions from the Arctic Ocean

Methane may be also emitted into the atmosphere from the coastal shelf containing submerged permafrost and methane hydrates. In particular gas hydrates contain large quantities of methane that are encapsulated under Arctic waters due to low water temperatures and high pressures at the bottom of the sea. Estimates of their impacts on methane emissions will be only briefly discussed here, because their formation is different than the formation of carbon deposits in the permafrost. The Arctic Ocean sea ice decline and warming of sea waters may provide conditions for partial release of methane from the ocean bottom. The impact of these conditions on the methane release is highly uncertain (AMAP 2015). Current model simulations with highly sophisticated models of ocean circulation and methane cycle in the ocean indicate, however, that the impact of Arctic Ocean warming on the marine methane release is going to be modest (Kirschke et al. 2013).

At present there is no clear evidence of major methane release from the Arctic Ocean into the atmosphere (James et al. 2016, Ruppel and Kessler 2017). In the future the changing environmental conditions adversely impact ocean-atmosphere fluxes (James et al. 2016, Ruppel and Kessler 2017). The loss of sea-ice may favour the stronger vertical mixing and larger fluxes into the atmosphere, while the higher stratification due to larger amount of fresh water at the ocean surface may decrease it. The higher stratification may, however, increase the warming of deeper layers and dissolve more methane in the water.

Although in the next decades major releases of methane stored in the Arctic Ocean into the atmosphere seem to be unlikely, their eventual realization could strongly accelerate global warming producing large economic impacts at the global scale (Whiteman et al. 2013). These economic estimates are, however, based on the assumption of the catastrophic release of methane from the Arctic Ocean, while the current complex modelling studies (e.g. Kirschke et al. 2013) indicate that the probability of such an event is very low.

4 Impact of permafrost degradation on infrastructures

Permafrost changes, such as reductions in thickness and/or spatial extent, determine disturbances in the land surface through different processes that can be summarized as:

- Thermokarst, subsidence of the ground surface and possible formation of a water body after thawing of ice-rich permafrost;
- Thermal erosion, wearing away of surface deposits by thermal and mechanical action;
- Coastal retreat, due to wave action in addition to water temperature (thermal abrasion), and warmer air temperature with permafrost thaw in the coastal bluffs affecting the destruction of coasts (thermal denudation);
- Permafrost-related slope processes, downslope movements of soil and rock near the surface, including slow movements such as frost creep and solifluction, and faster movements such as landslides;
- Frost heave, upward movement of the ground due to freezing of water in the soil and formation of ice lenses.

These processes associated to permafrost thawing impact the communities, urban environments and infrastructure networks in the Arctic, with different issues involved in different regions (Hjort et al. 2018). At the same time construction and operation of an infrastructure can affect permafrost in complex ways. Furthermore, increasing industrial and development activities in the Arctic will probably increase in the future due to increasing demand of natural resources and easier access to land areas in the Arctic as a consequence of declining sea ice and glaciated land areas becoming ice free. To assess the impacts of climate change on anthropogenic systems is highly uncertain due to the uncertainties of climate projections and the human intervention with permafrost soils, which may outweigh the effect of climate change (AMAP 2017).

The RATIC (Rapid Arctic Transitions due to Infrastructure and Climate) initiative identified the impacts of permafrost thawing on natural and built environment as priority issues across the entire Arctic, with regional differences (Walker and Peirce, 2015).

In Alaska the cumulative effects of infrastructure and climate on permafrost was analysed for example in the Prudhoe Bay oilfield, which was developed since 1968 and now composed by about infrastructure items (e.g. drill and exploration sites, support and production pads), a network of roads and causeways of about 1000 km, and a total area affected of more than 70 km². The direct effects (e.g. gravel pads, excavations, roads, and pipelines) cover about 15% of the mapped area, while indirect effects (e.g. flooding and thermokarst related to the infrastructure and climate change) cover about the double the area of direct effects, with implications for the ecosystems and for the social system and adaptive management of infrastructure expansion.

In Russia the Bovanenkovo gas field in the Yamal Peninsula covers an area of about 40 km² in terms of permanent infrastructures, but the visibly affected area estimated from remote sensing imagery spans over almost 1000 km². In this region permafrost changes generated landslides and thermos-denudation of slopes, which created highly dissected landscapes, with present hazards for gas extraction and other land uses. Furthermore, the petroleum industry expansion, permafrost melting, increasing shrubification, and other impacts of climate change, such as changing precipitation patterns, pose at risk the traditional reindeer/herding Nenets way of life in the Yamal Peninsula. The bearing capacity of a standard foundation pile imbedded in permafrost was measured and analysed in different regions in Siberia (Strelletsaki et al., 2012a,b). Observational data show that the foundation bearing capacity, in the period 2000-2010 compared to the year of construction (1960s), decreased on average by 12% (up to 37% in Western Siberia, 26% in Central Siberia, and 48% in Eastern Siberia). Considering the impacts on permafrost in a future climate (RCP8.5 scenario), the projected bearing capacity in 2050 using six climate models decrease up to 67±28%. By evaluating six CMIP5 predictions, Shiklomanov et al. (2016) estimate that in the first half of the 21st century climate change will reduce urban infrastructure stability over the Russian permafrost by at least 25%, although there is a significant difference in estimates originating from different CMIP5 models.

In Canada 50% of the landmass is underlain by permafrost, and the integrity of many ecosystems and infrastructures depends on the stability of these frozen lands. Increased active layer depth and more frequent slope processes in the continuous permafrost region and more frequent thermokarst in the discontinuous permafrost region are changing the landscape in northern Canada. The impacts also on water bodies, soil drainage and vegetation affect resources traditionally available for humans, among others drinking water sources. Also the infrastructures that support public safety and economic activities are greatly affected in a period of increasing socio-economic development of the Canadian Arctic, mainly related to the oil, gas and

mining industry. Recently two large scale research projects in Canada address the processes and implications of permafrost thawing and degradation: ADAPT (Arctic Development and Adaptation to Permafrost in Transition) and the IRIS (Integrated Regional Impact Studies) of the ArcticNet project.

In Scandinavia future climate projections estimate milder winters. Stable winter conditions will be more likely replaced by several freeze/thaw cycles and frost heave, impacting mainly the roads network with increasing maintenance costs (Grendstad 2012).

5 Conclusions

The strong magnification of global warming in the Arctic amplifies the rate of thawing of permafrost. This process could produce a positive feedback to the global warming by emitting carbon into the atmosphere in the form of methane (CH_4) and carbon dioxide (CO_2). Furthermore, the existing and future construction on the permafrost area may be endangered by movements of the soil due to its thawing. This study evaluates climate change impacts on the permafrost by reviewing the existing literature and estimating future impacts simulated by three CMIP5 ensemble simulations forced by the three RCP scenarios.

By combining information from the literature on global warming trends and evaluating CMIP5 simulations it is concluded that Arctic amplification of global warming in the last decades is mainly due to warming over ocean and sea-ice in winter and over land in summer, while during the last decades there are no significant positive trends of near-surface temperatures over land in winter. In the last decades summer trends of near-surface temperature over land in the Arctic are positive and similar to trends over global land areas.

CMIP5 simulations correctly estimate yearly averaged global warming, while the Arctic amplification is attenuated due to the lower rise of temperature over the Arctic Ocean. During the 21st century over land in the Arctic CMIP5 simulations show warming in winter and no trend in summer, that is opposite from observed seasonal trends. The disagreement between CMIP5 simulations in the seasonal distribution of warming trends may partly explain the inability of CMIP5 simulations to capture the magnitude of Arctic warming, because the major impact on permafrost thawing should be in summer when atmospheric near-surface temperatures rise above zero degrees.

Based on the available literature, it may be estimated that in the 21st century additional methane emissions from the Arctic permafrost on the land may be approximately 10-15 Tg/y. Additional methane release from the continental shelf in the Arctic Ocean during the 21st century is very uncertain, while current emission estimates vary from 1 to 17 Tg/y. When compared to other sources globally, most probably these rates of methane emissions may not significantly impact the global warming rate in the 21st century. However, there may be events of sudden releases with strong global impacts that are difficult to predict.

By evaluating available literature, atmospheric reanalysis and CMIP5 simulations it can be estimated that in the last three decades, an increasing quantity of carbon present in the permafrost has become available for the microbial decomposition. CMIP5 simulations agree with atmospheric reanalyses in estimating trends of carbon availability for the microbial decomposition. In agreement with other studies, we estimate that in the 21st century permafrost will totally emit from the stored carbon about 80 Pg C in RCP 2.6, 85 Pg C in RCP 4.5 and 97 Pg C in RCP 8.5 scenario. These values are about 10% of current total anthropogenic emissions estimated at approximately 10 Gt/y.

On the other hand, a number of studies indicate that carbon content in the permafrost will increase due to the development of vegetation. During the first part of the 21st century sequestration of carbon by new vegetation may be faster than depletion of carbon stored in the permafrost. Towards the end of the 21st century permafrost will become a source of atmospheric carbon, but depletion of the present carbon in the permafrost may be partly compensated by depositions and storage from the new vegetation. Depending on the RCP scenario, in the 21st century the lowest total carbon emissions from permafrost are estimated to be less than 12 Pg. Emissions of that order of magnitude would not have a significant impact on global warming by anthropogenic CO_2 emissions. These estimates are, however, based on models that cannot fully resolve all processes relevant for the development of the new vegetation over the permafrost and may overestimate carbon sinks. More recent studies indicate that the offset of emissions by new vegetation may be much less significant. In this case future carbon emissions from the permafrost due to global warming may become comparable to current anthropogenic emissions.

The effects of permafrost thawing on ecosystems and infrastructures at the local and regional scale are still highly uncertain, despite the current general understanding of the processes driving the past and future changes in the permafrost. The main challenge to address is the limited knowledge of local processes with a sufficient spatial and temporal coverage, which can be tackled only by using a combination of field studies, remote sensing analysis and modelling approaches. The impacts on the indigenous people of the Arctic due to resource development and fragmentation of large ecosystems (by roads, railways and pipelines) must be taken into account as well (AMAP 2017).

The reduction of global warming envisaged by the Paris agreement will require diminishing of anthropogenic emissions already in the first half of the 21st century. In this case potential CO_2 emissions from the permafrost thawing may overcome anthropogenic emissions and Paris agreement targets to reduce the global warming

may be exceeded sooner than expected. The additional emission of CO₂ and CH₄ caused by this natural process triggered by warming in the high latitudes will diminish the budget of CO₂ humankind can emit to keep below the agreed level of global warming requiring additional efforts for the mitigation of global warming.

The results of this report may support the EU policy for the Arctic by providing additional evidence on the changing Arctic permafrost and presenting the range of estimates for emissions of CO₂ and CH₄ in the 21st century. The results may also provide a scientific contribution to the EU efforts in implementing the Paris agreement goals. In particular, they may support the EU science policy in the Arctic by emphasizing the need for the long term monitoring and predicting of permafrost thawing and its emissions of greenhouse gasses, in order to reduce the currently large uncertainties in estimating future impacts of permafrost thawing on climate change. The study may support the EU efforts in developing the international cooperation in the Arctic by providing additional evidence on regional and global effects of the enhanced arctic warming. In this way the report may provide a valuable input for the Northern Dimension policy and the EU participation in AMAP Working Groups.

The methodology developed in the report for estimating present and future emissions of CO₂ from the thawing permafrost used currently available input data on emission rates and future change of global and regional temperatures. In the future the same methodology may be used with new scientific estimates of the emission rates and different climate scenarios including those that are more stringent than the Paris agreement.

References

- Abbott, B. W., et al., 2016, Biomass offsets little or none of permafrost carbon release from soils, streams, and wildfire: an expert assessment, *Environ Res Lett*, 11, 1–13, doi:10.1088/1748-9326/11/3/034014.
- AMAP Assessment, 2015: Methane as an Arctic climate forcer. Arctic Monitoring and Assessment Programme (AMAP), Oslo, Norway. vii + 139 pp.
- AMAP, 2017. Snow, Water, Ice and Permafrost in the Arctic (SWIPA) 2017. Arctic Monitoring and Assessment Programme (AMAP), Oslo, Norway. xiv + 269 pp.
- Årthun, M., M. Eldevik, L. H. Smedsrød, Ø. Skagseth, and R. B. Ingvaldsen, 2012, Quantifying the Influence of Atlantic Heat on Barents Sea Ice Variability and Retreat, *J. Climate* 25, 4736–4743, doi:10.1175/JCLI-D-11-00466.1.
- Bergamaschi, P. et al., 2013. Atmospheric CH₄ in the first decade of the 21st century: Inverse modeling analysis using SCIAMACHY satellite retrievals and NOAA surface measurements. *Journal of Geophysical Research: Atmospheres*, 118:7350-7369.
- Biskaborn, B. K. et al., 2019, Permafrost is warming at a global scale, *Nature Comm.*, 1–11, doi:10.1038/s41467-018-08240-4.
- Blunden, J., and D. S. Arndt, Eds., 2017: State of the Climate in 2016. *Bull. Amer. Meteor. Soc.*, 98 (8), Si–S277, doi:10.1175/2017BAMSSStateoftheClimate.1.
- Bousquet, P., P. Ciais, J.B. Miller, E.J. Dlugokencky, D.A. Hauglustaine, C. Prigent, G.R. Van der Werf, P. Peylin, E.-G. Brunke, C. Carouge, R.L. Langenfelds, J. Lathière, F. Papa, M. Ramonet, M. Schmidt, L.P. Steele, S.C. Tyler and J. White, 2006. Contribution of anthropogenic and natural sources to atmospheric methane variability. *Nature*, 443:439-443.
- Burke, E. J., C. D. Jones, and C. D. Koven, 2013, Estimating the Permafrost-Carbon Climate Response in the CMIP5 Climate Models Using a Simplified Approach, *J Climate*, 26(14), 4897–4909, doi:10.1175/JCLI-D-12-00550.1.
- Cao, M., S. Marshall and K. Gregson, 1996. Global carbon exchange and methane emissions from natural wetlands: Application of a process-based model. *Journal of Geophysical Research*, 101:14,399-14,414.
- Ciais, P, Sabine, C, Bala, G, Bopp, L, Brovkin, V, al., E & House, JI 2013, Carbon and Other Biogeochemical Cycles: Climate Change 2013: The Physical Science Basis. Contribution of Working Group I to the Fifth Assessment Report of the Intergovernmental Panel on Climate Change Change. in O Edenhofer, R Pichs-Madruga, Y Sokona, E Farahani, S Kadner, K Seyboth, A Adler, I Baum, S Brunner, P Eickemeier, B Kriemann, J Savolainen, S Schröder, C von Stechow, Z T. & M J.C. (eds), Climate Change 2013: The Physical Science Basis. Contribution of Working Group I to the Fifth Assessment Report of the Intergovernmental Panel on Climate Change Change. Cambridge University Press, Cambridge, United Kingdom and New York, NY, USA.
- Clarke, A. D., and K. J. Noone, 1985, Soot in the Arctic snowpack: a cause for perturbations in radiative transfer, *Atmos. Env.*, 19, 2045-2053.
- Clarke, L., J. Edmonds, H. Jacoby, H. Pitcher, J. Reilly, R. Richels, 2007. Scenarios of Greenhouse Gas Emissions and Atmospheric Concentrations. Sub-report 2.1A of Synthesis and Assessment Product 2.1 by the U.S. Climate Change Science Program and the Subcommittee on Global Change Research. Department of Energy, Office of Biological & Environmental Research, Washington, 7 DC., USA, 154 pp.
- Dee, D. P., et al., 2011, The ERA-Interim reanalysis: Configuration and performance of the data assimilation system. *Quart. J. Roy. Meteor. Soc.*, 137, 553–597, doi:10.1002/qj.828.
- Ding, Q., J. M. Wallace, D. S. Battisti, E. J. Steig, A. J. E. Gallant, H.-J. Kim, and L. Gei (2014), Tropical forcing of the recent rapid Arctic warming in northeastern Canada and Greenland, *Nature*, 509, 209–12, doi:10.1038/nature13260.
- Dlugokencky, E. J., et al., 2009. Observational constraints on recent increases in the atmospheric CH₄ burden. *Geophysical Research Letters*, 36:L18803, doi:10.1029/2009GL039780.
- Fujino, J., R. Nair, M. Kainuma, T. Masui, Y. Matsuoka, 2006. Multi-gas mitigation analysis on stabilization scenarios using AIM global model. *Multigas Mitigation and Climate Policy. The Energy Journal Special Issue*.

- Grant, R.F., 1998. Simulation of methanogenesis in the mathematical model ecosys. *Soil Biology and Biochemistry*, 30:883-896.
- Grendstad, G., editor. 2012. Adaptation to climate change. Conference o fEuropean Directors of Roads, CEDR Secretariat General, Paris, France.
- Hijjoka, Y., Y. Matsuoka, H. Nishimoto, M. Masui, and M. Kainuma, 2008. Global GHG emissions scenarios under GHG concentration stabilization targets. *Journal of Global Environmental Engineering* 13, 97-108.
- Hjort, J., O. Karjalainen, J. Aalto, S. Westermann, V. E. Romanovsky, F. E. Nelson, B. Etzelmüller, and M. Luoto (2018), Degrading permafrost puts Arctic infrastructure at risk by mid-century, *Nature Comm.*, 1–9, doi:10.1038/s41467-018-07557-4.
- Hope, C., and K. Schaefer, 2015, Economic impacts of carbon dioxide and methane released from thawing permafrost, *Nature Clim. Ch.*, 6, 56–59, doi:10.1038/nclimate2807.
- Houweling, S., et al., 2014. A multi-year methane inversion using SCIAMACHY, accounting for systematic errors using TCCON measurements. *Atmospheric Chemistry and Physics*, 14:3991-4012.
- Hugelius, G. et al., 2014, Estimated stocks of circumpolar permafrost carbon with quantified uncertainty ranges and identified data gaps, *Biogeosciences*, 11(23), 6573–6593, doi:10.5194/bg-11-6573-2014.
- James, R. H., et al., 2016, Effects of climate change on methane emissions from seafloor sediments in the Arctic Ocean: A review. *Limnol. Oceanogr.*, 61: S283–S299. doi:10.1002/lno.10307
- Kalnay, E., et al., 1996, The NCEP/NCAR 40-Year Re- analysis Project. *Bull. Amer. Meteor. Soc.*, 77, 437–471, doi:10.1175/1520-0477(1996)077,0437:TNYRP.2.0.CO;2.
- Kashiwase, H., K. I. Ohshima, S. Nihashi, and H. Eicken (2017), Evidence for ice-ocean albedo feedback in the Arctic Ocean shifting to a seasonal ice zone, *Sci. Rep.*, 1–10, doi:10.1038/s41598-017-08467-z.
- Kirschke, S., et al., 2013. Three decades of global methane sources and sinks. *Nature Geoscience*, 6:813–823.
- Koven, C. D., Ringeval, B., Friedlingstein, P., Ciais, P., Cadule, P., Khvorostyanov, D., Krinner, G., and Tarnocai, C.: Permafrost carbon-climate feedbacks accelerate global warming, *P. Natl. Acad. Sci.*, 108, 14769–14774, doi:10.1073/pnas.1103910108, 2011.
- Koven, C. D., W. J. Riley, and A. Stern, 2013, Analysis of Permafrost Thermal Dynamics and Response to Climate Change in the CMIP5 Earth System Models, *J Climate*, 26(6), 1877–1900, doi:10.1175/JCLI-D-12-00228.1.
- McGuire, A.D., et al., 2012. An assessment of the carbon balance of Arctic tundra: comparisons among observations, process models, and atmospheric inversions. *Biogeosciences*, 9:3185–3204.
- Moore, T.R. and N.T. Roulet, 1993. Methane flux–water-table relations in northern wetlands. *Geophysical Research Letters*, 20:587–590.
- Nitze, I., G. Grosse, B. M. Jones, V. E. Romanovsky, and J. Boike, 2018, Remote sensing quantifies widespread abundance of permafrost region disturbances across the Arctic and Subarctic, *Nature Communications*, 1–11, doi:10.1038/s41467-018-07663-3.
- Osterkamp, T. E., and C. R. Burn, 2003, Permafrost, in *Encyclopedia of Atmospheric Sciences*, edited by J. R. Holton, pp. 1717–1729, Academic, Oxford, U. K., doi:10.1016/B0-12-227090-8/00311-0.
- Peings, Y., and G. Magnusdottir, 2014, Forcing of the wintertime atmospheric circulation by the multidecadal fluctuations of the North Atlantic ocean, *Environ. Res. Lett.* 9(3), 034018, doi: 10.1088/1748-9326/9/3/034018.
- Perlitz, J., Hoerling, M., and R. Dole, 2015, Arctic Tropospheric Warming: Causes and Linkages to Lower Latitudes, *J. Clim.* 28(6), 2154–2167, doi:10.1175/JCLI-D-14-00095.1.
- Petrescu, A.M.R., et al., 2010. Modeling regional to global CH₄ emissions of boreal and arctic wetlands. *Global Biogeochemical Cycles*, 24: GB4009, doi:10.1029/2009GB003610.
- Pithan, F., and T. Mauritsen, 2014, Arctic amplification dominated by temperature feedbacks in contemporary climate models, *Nat. Geosci.* 7, 2–5, doi:10.1038/NGEO2071.
- Potter, C.S. and S.A. Klooster, 1997. Global model estimates of carbon and nitrogen storage in litter and soil pools: response to changes in vegetation quality and biomass allocation. *Tellus*, 49B:1–17.
- Poulter, B., et al., 2017, Global wetland contribution to 2000–2012 atmospheric methane growth rate dynamics, *Environ Res Lett*, 12, 094013–16, doi:10.1088/1748-9326/aa8391.

- Prather, M.J., C.D. Holmes and J. Hsu, 2012. Reactive greenhouse gas scenarios: Systematic exploration of uncertainties and the role of atmospheric chemistry. *Geophysical Research Letters*, 39:L09803, doi:10.1029/2012GL051440.
- Revich, B. A., et al., 2011, Thawing of permafrost may disturb historic cattle burial grounds in East Siberia, *Global Health Action*, 4, doi:10.3402/gha.v4i0.8482.
- Riahi, K. Gruebler, A. and Nakicenovic N.: 2007. Scenarios of long-term socio-economic and environmental development under climate stabilization. *Technological Forecasting and Social Change* 74, 7, 887-935.
- Ruppel, C. D., and J. D. Kessler 2017, The interaction of climate change and methane hydrates, *Rev. Geophys.*, 55, 126-168, doi:10.1002/2016RG000534.
- Schaphoff, S., Heyder, U., Ostberg, S., Gerten, D., Heinke, J., and Lucht, W.: Contribution of permafrost soils to the global carbon budget, *Environ. Res. Lett.*, 8, 014026, <http://stacks.iop.org/1748-9326/8/i=1/a=014026>, 2013.
- Serreze, M. C., and J. A. Francis, 2006, The arctic amplification debate, *Climatic Change*, 76, 241–264, doi: 10.1007/s10584-005-9017-y.
- Schuster, P. F., et al., 2018, Permafrost stores a globally significant amount of mercury. *Geophys. Res. Lett.*, 45. <https://doi.org/10.1002/2017GL075571>
- Schuur, E. A. G. et al., 2015: Climate change and the permafrost carbon feedback. *Nature*, 520, 171-179, Doi:10.1038/nature14338
- Shiklomanov, N. I., D. A. Streletskiy, T. B. Swales, and V. A. Kokorev, 2016, Climate Change and Stability of Urban Infrastructure in Russian Permafrost Regions: Prognostic Assessment based on GCM Climate Projections, *Geogr. Rev.*, 107, 125–142, doi:10.1111/gere.12214.
- Streletskiy, D.A., N.I. Shiklomanov and E. Hatleberg, 2012a. Infrastructure and a changing climate in the Russian Arctic: A geographic impact assessment. *Proceedings of the Tenth International Conference on Permafrost*, 25–29 June, Salekhard, Russia, 1:407–414.
- Streletskiy, D.A., N.I. Shiklomanov and F.E. Nelson, 2012b. Permafrost, infrastructure, and climate change: A GIS-based landscape approach to geotechnical modelling. *Arctic, Antarctic, and Alpine Research*, 44:368–380.
- Taylor, K.E., R.J. Stouffer and G.A. Meehl, 2012. An Overview of CMIP5 and the experiment design. *Bulletin of the American Meteorological Society*, 93:485–498.
- van Vuuren, D., M. den Elzen, P. Lucas, B. Eickhout, B. Strengers, B. van Ruijven, S. Wonink, R. van Houdt, 2007. Stabilizing greenhouse gas concentrations at low levels: an assessment of reduction strategies and costs. *Climatic Change*, doi:10.1007/s10584-006-9172-9.
- Voigt, C., et al., 2017, Increased nitrous oxide emissions from Arctic peatlands after permafrost thaw. *Proceedings of the National Academy of Sciences*, 114, 6238–6243.
- Walker, D.A. and J. Pierce (eds.), 2015. Rapid Arctic Transitions due to Infrastructure and Climate (RATIC): A contribution to ICARP III. Alaska Geobotany Center, University of Alaska Fairbanks.
- Whiteman, G., C. Hope and P. Wadhams, 2013, Vast costs of Arctic change, *Nature*, 499, 401–403.
- Wise, MA, KV Calvin, AM Thomson, LE Clarke, B Bond-Lamberty, RD Sands, SJ Smith, AC Janetos, JA Edmonds. 2009. Implications of Limiting CO₂ Concentrations for Land Use and Energy. *Science*. 324:1183–1186. May 29, 2009.
- WMO, 2014. WMO statement on the status of the global climate in 2013. WMO-No. 1130, World Meteorological Organization, Geneva, Switzerland.
- Zhang, W., et al., 2013. Tundra shrubification and tree-line advance amplify arctic climate warming: results from an individual-based dynamic vegetation model. *Environmental Research Letters*, 8:034023, doi:10.1088/1748-9326/8/3/034023.

List of abbreviations and definitions

ADAPT	Arctic Development and Adaptation to Permafrost in Transition
AMAP	Arctic Monitoring and Assessment Programme
AR5	Fifth Assessment Report
CESM	Community Earth System Model
CH ₄	Methane
CMIP5	Coupled Model Intercomparison Project version 5
CO ₂	Carbon dioxide
EC	European Commission
ECMWF	European Centre for Medium-Range Weather Forecasts
EDGAR	Emissions Database for Global Atmospheric Research
EEAS	European External Action Service
IRIS	Integrated Regional Impact Studies
IPCC	Intergovernmental Panel on Climate Change
IPSL	Institut Pierre Simon Laplace
MPI	Max Planck Institute
NCEP	National Centers for Environmental Prediction
NOAA	National Oceanic and Atmospheric Administration
RATIC	Rapid Arctic Transitions due to Infrastructure and Climate
RF	Radiative Forcing
RCP	Representative Concentration Pathway
SST	Sea Surface Temperature
WMO	World Meteorological Organization

List of boxes

Box 1. Permafrost and estimated carbon content in frozen soil	4
Box 2. Estimates of temperature trends	8
Box 3. Atmospheric reanalysis	9
Box 4. CMIP5 and RCPs.....	13
Box 5. Global estimates of methane emissions	21

List of figures

Figure 1. Land area covered by permafrost north of 45°N based on data from Hugelius et al (2014).....	3
Figure 2. Schematic representation of vertical temperature profiles of permafrost layers (the figure is an adaptation from Figure 1 of Osterkamp and Burn, 2003).	4
Figure 3. Carbon content (kg C/m ²) in the near surface layer of permafrost within the depth of 3 meters based on data from Hugelius et al (2014).....	5
Figure 4. Linear trend of near-surface temperature in winter (December–January–February) (°C/decade) between 1980 and 2015. a) ERA-INTERIM reanalysis and b) NCEP reanalysis.	9
Figure 5. Linear trend of near-surface temperature in summer (June–July–August) (°C/decade) between 1980 and 2015. a) ERA-INTERIM reanalysis and b) NCEP reanalysis.....	10
Figure 6. CESM ensemble mean of near-surface temperature change in the RCP2.6 scenario: yearly averaged global temperature (green), yearly averaged temperature north of 60°N (black), winter (January–February–March) averaged temperature north of 60°N (red) and summer (June–July–August) averaged temperature north of 60°N (blue). Panel a shows averages over land and ocean, and panel b averages only over land.	11
Figure 7. Same as Fig. 6, but for RCP 8.5 scenario.	11
Figure 8. Estimated carbon content in the permafrost (Pg) in summer (June–July–August) between 1980 and 2015: a) inside the active layer and b) in the soil with temperatures higher than 5 °C. Soil temperatures are estimated by ERA-INTERIM reanalysis (full black), NCEP reanalysis (dashed black), mean of 6 CESM CMIP5 simulations (green), mean of 3 IPSL CMIP5 simulations (red) and mean of 3 MPI CMIP5 simulations (cyan). CMIP5 simulations used historical forcing between 1980 and 2005, and RCP 2.6 forcing after 2005.	15
Figure 9. Estimated carbon content in permafrost (Pg) in summer (June–July–August) between 2006and 2100: a) inside the active layer and b) in the soil with temperatures higher than 5 °C. Soil temperatures are estimated by ERA-INTERIM reanalysis (full black), NCEP reanalysis (dashed black), mean of 6 CESM CMIP5 simulations (green), mean of 3 IPSL CMIP5 simulations (red) and mean of 3 MPI CMIP5 simulations (cyan). CMIP5 simulations were forced by RCP 2.6 scenario.	15
Figure 10. Linear trends of carbon content (Pg C/y) at temperatures above 0 °C (top) and above 5 °C (bottom) in the historical period (1986–2005) and for the three RCP scenarios in the 21 st century (2006–2100). All trends are statistically significant at 0.05 value. Trends do not contain estimates of microbial activity.	17
Figure 11. Emissions into atmosphere of carbon present in the permafrost (Pg C/y): a) RCP 2.6, b) RCP 4.5 and c) RCP 8.5. Ensemble means are represented by green (CESM), red (IPSL) and cyan (MPI) lines.	18
Figure 12. Anomalies of near-surface temperature (°C) with respect to 1980–1989 mean in the ERA-INTERIM reanalysis: winter (January–February–March) averaged global temperature (black full), winter averaged temperature north of 60°N (black dashed), summer (June–July–August) averaged global temperature (green solid curve) and summer averaged temperature north of 60°N (green dashed). Panel a shows averages over land and ocean, and panel b averages only over land.	36
Figure 13. Anomalies of near-surface temperature (°C) with respect to 1980–1989 mean in the NCEP reanalysis: winter (January–February–March) averaged global temperature (black full), winter averaged temperature north of 60°N (black dashed), summer (June–July–August) averaged global temperature (green full) and summer averaged temperature north of 60°N (green dashed). Panel a shows averages over land and ocean, and panel b averages only over land.	36
Figure 14. CESM ensemble mean of the change of near-surface temperature in CMIP5 scenarios: winter (January–February–March) averaged global temperature (full-black), winter averaged temperature north of 60°N (dashed-black), summer (June–July–August) averaged global temperature (full-green) and summer averaged temperature north of 60°N (dashed-green). Panel a shows averages over land and ocean in RCP 2.6, panel b averages only over land in RCP 2.6, panel c averages over land and ocean in RCP 8.5, and panel d averages only over land in RCP 8.5.	37
Figure 15. Same as Fig. 9, but for RCP 4.5 scenario.	38
Figure 16. Same as Fig. 9, but for RCP 8.5 scenario.	38

Figure 17. Panels a-c show estimated change of carbon content in permafrost (hg/m ²) in summer (June-July-August) between periods 2006-2100 under the RCP 2.6 scenario and 1986-2005 at temperatures above 0 °C: a) mean of 6 CESM CMIP5 simulations, b) mean 3 IPSL CMIP5 simulations and c) mean of 3 MPI CMIP5 simulations. Panels d-f show estimated change at temperatures above 5 °C: d) mean of 6 CESM CMIP5 simulations, e) mean 3 IPSL CMIP5 simulations and d) mean of 3 MPI CMIP5 simulations.	39
Figure 18. Same as Fig. 17, but for RCP 4.5 scenario.....	40
Figure 19. Same as Fig. 17, but for RCP 8.5 scenario	41
Figure 20. Same as Fig. 11, but for the 0.5% degradation rate.....	42
Figure 21. Same as Fig. 11, but for the 1.5% degradation rate.....	42

List of tables

Table 1. Difference between mean carbon content (Pg) estimated by CMIP5 simulations in periods 2006–2100 and 1986–2005. Differences are made for carbon content at temperatures above 0 °C and 5 °C. Values are given for each CMIP5 ensemble and for the average among all three ensembles.....	17
Table 2. Partition of contributions of anthropogenic sources to annual emissions for the period 2000–2009 (Kirschke et al. 2013; Saunois et al., 2016)	22
Table 3. Partition of contributions of natural sources to annual emissions for the period 2000–2009 (Kirschke et al. 2013), and 2003–2012 (Saunois et al., 2016)	23

Annexes

Annex 1. Supplementary figures

Figure 12. Anomalies of near-surface temperature ($^{\circ}\text{C}$) with respect to 1980-1989 mean in the ERA-INTERIM reanalysis: winter (January–February–March) averaged global temperature (black full), winter averaged temperature north of 60°N (black dashed), summer (June–July–August) averaged global temperature (green solid curve) and summer averaged temperature north of 60°N (green dashed). Panel a shows averages over land and ocean, and panel b averages only over land.

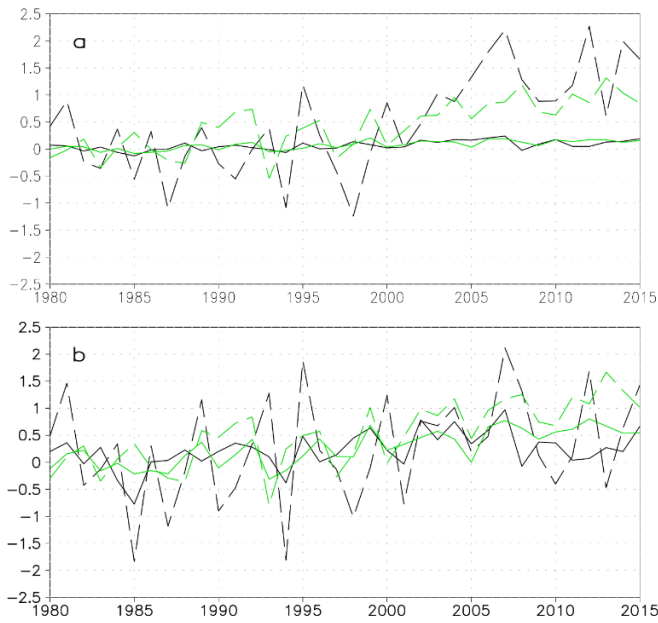


Figure 13. Anomalies of near-surface temperature ($^{\circ}\text{C}$) with respect to 1980-1989 mean in the NCEP reanalysis: winter (January–February–March) averaged global temperature (black full), winter averaged temperature north of 60°N (black dashed), summer (June–July–August) averaged global temperature (green full) and summer averaged temperature north of 60°N (green dashed). Panel a shows averages over land and ocean, and panel b averages only over land.

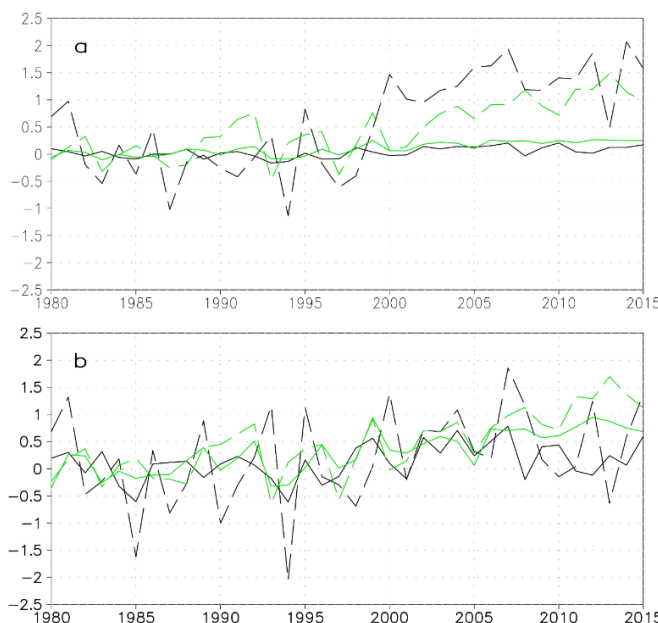


Figure 14. CESM ensemble mean of the change of near-surface temperature in CMIP5 scenarios: winter (January–February–March) averaged global temperature (full-black), winter averaged temperature north of 60°N (dashed-black), summer (June–July–August) averaged global temperature (full-green) and summer averaged temperature north of 60°N (dashed-green). Panel a shows averages over land and ocean in RCP 2.6, panel b averages only over land in RCP 2.6, panel c averages over land and ocean in RCP 8.5, and panel d averages only over land in RCP 8.5.

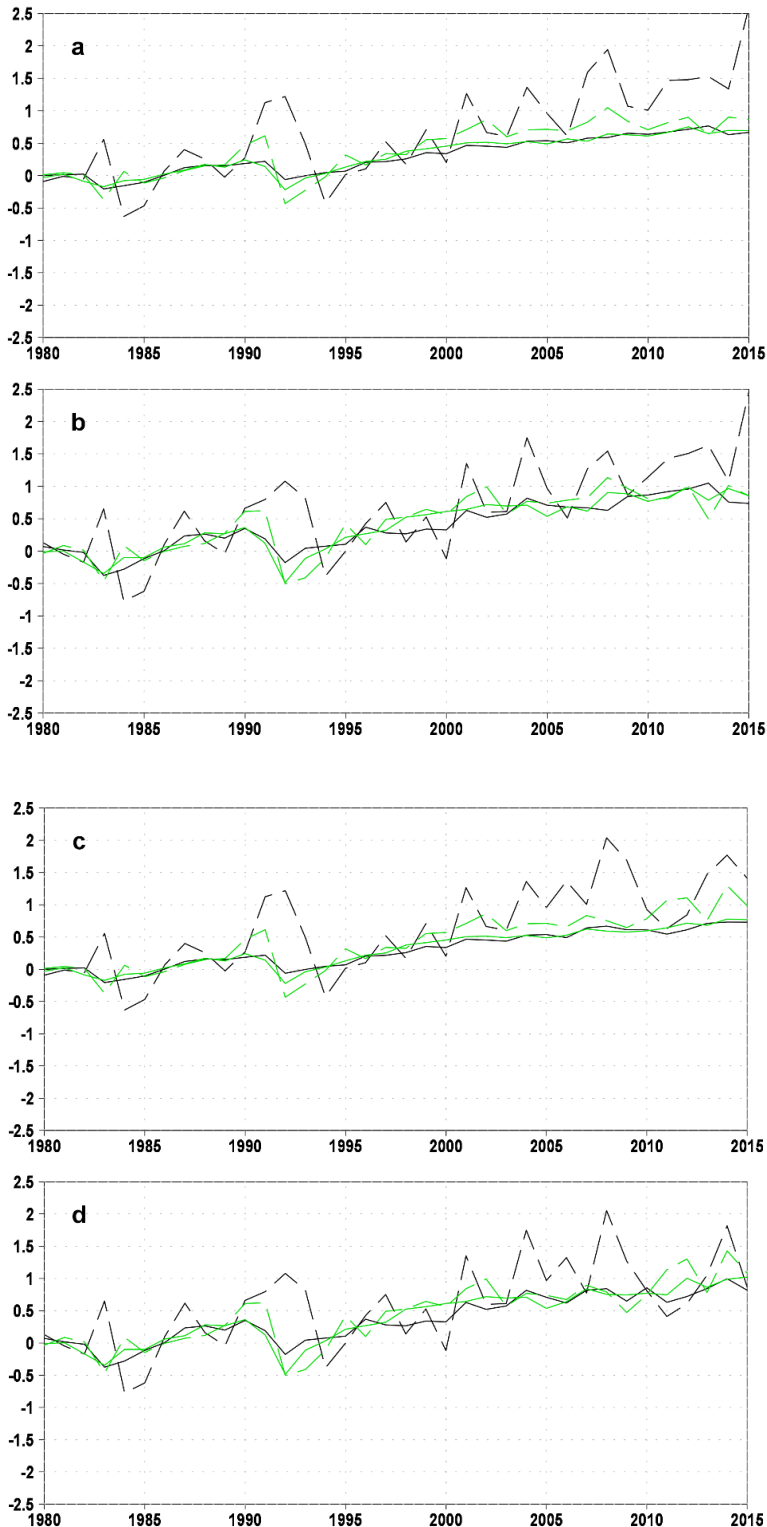


Figure 15. Same as Fig. 9, but for RCP 4.5 scenario.

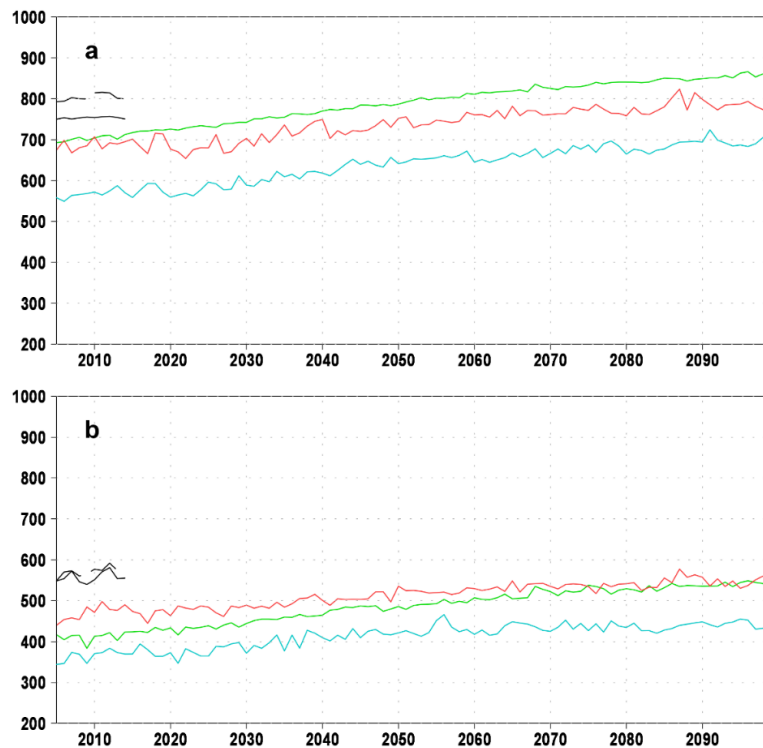


Figure 16. Same as Fig. 9, but for RCP 8.5 scenario.

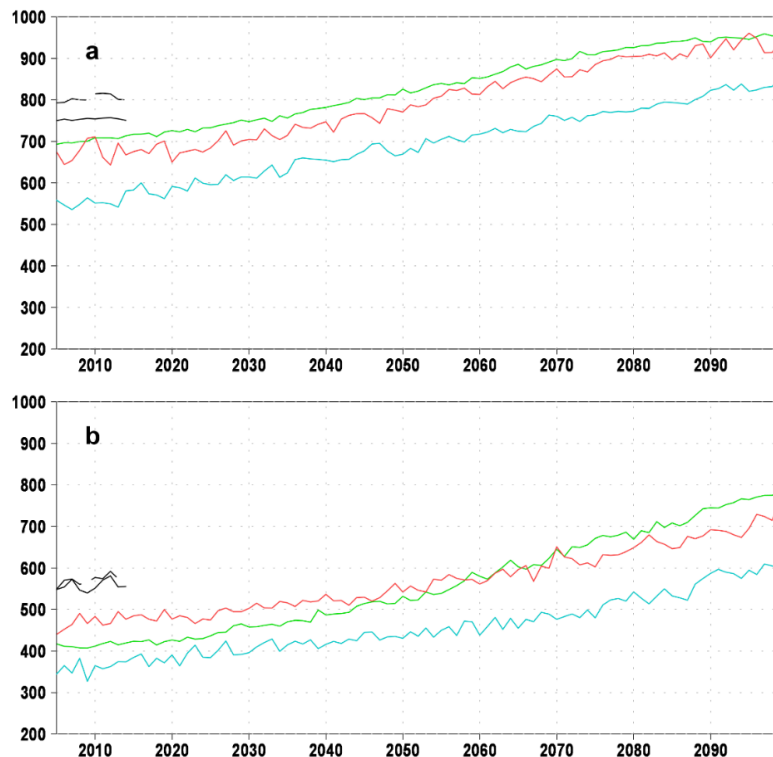


Figure 17. Panels a-c show estimated change of carbon content in permafrost (hg/m²) in summer (June–July–August) between periods 2006–2100 under the RCP 2.6 scenario and 1986–2005 at temperatures above 0 °C: a) mean of 6 CESM CMIP5 simulations, b) mean 3 IPSL CMIP5 simulations and c) mean of 3 MPI CMIP5 simulations. Panels d-f show estimated change at temperatures above 5 °C: d) mean of 6 CESM CMIP5 simulations, e) mean 3 IPSL CMIP5 simulations and f) mean of 3 MPI CMIP5 simulations.

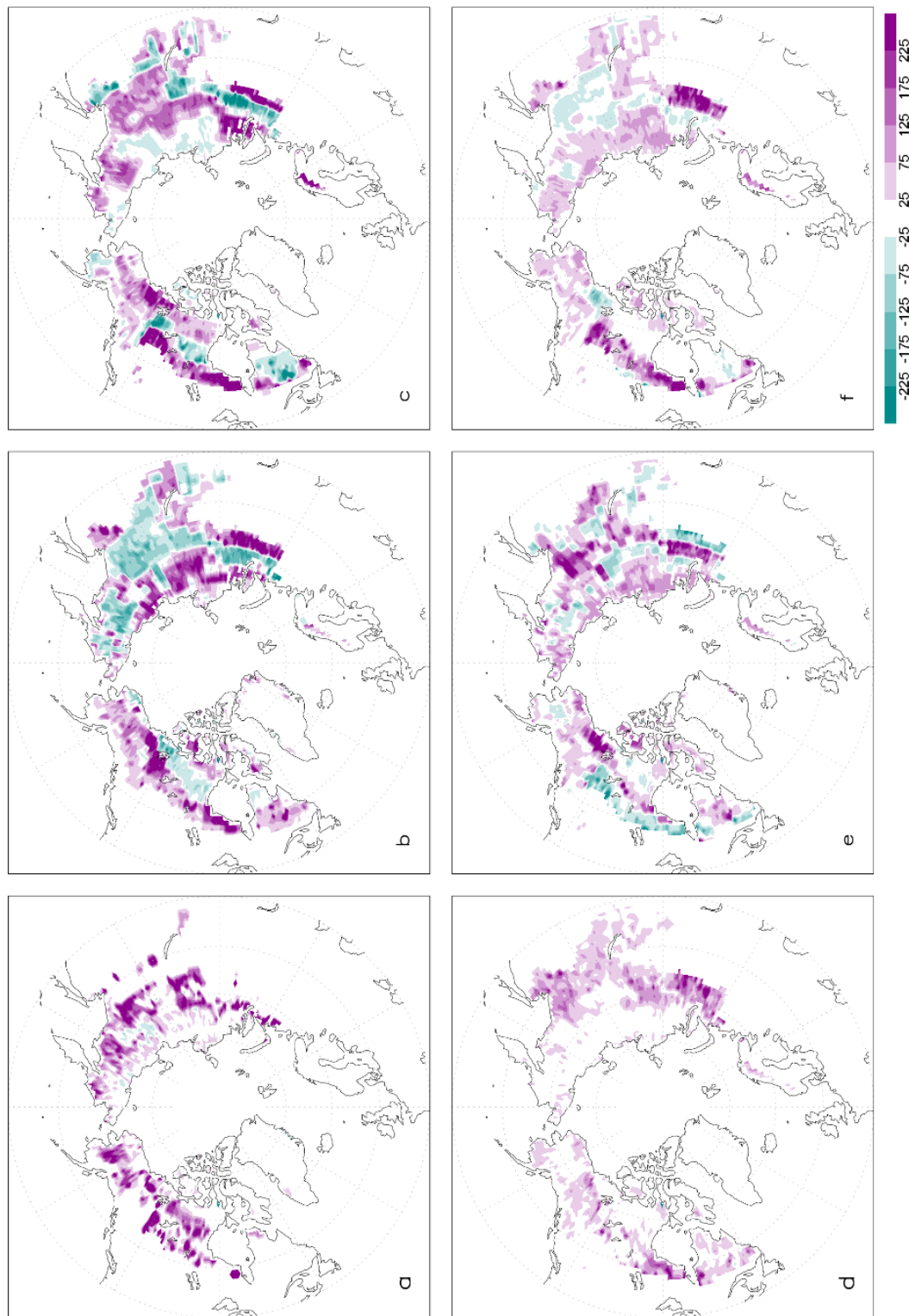


Figure 18. Same as Fig. 17, but for RCP 4.5 scenario.

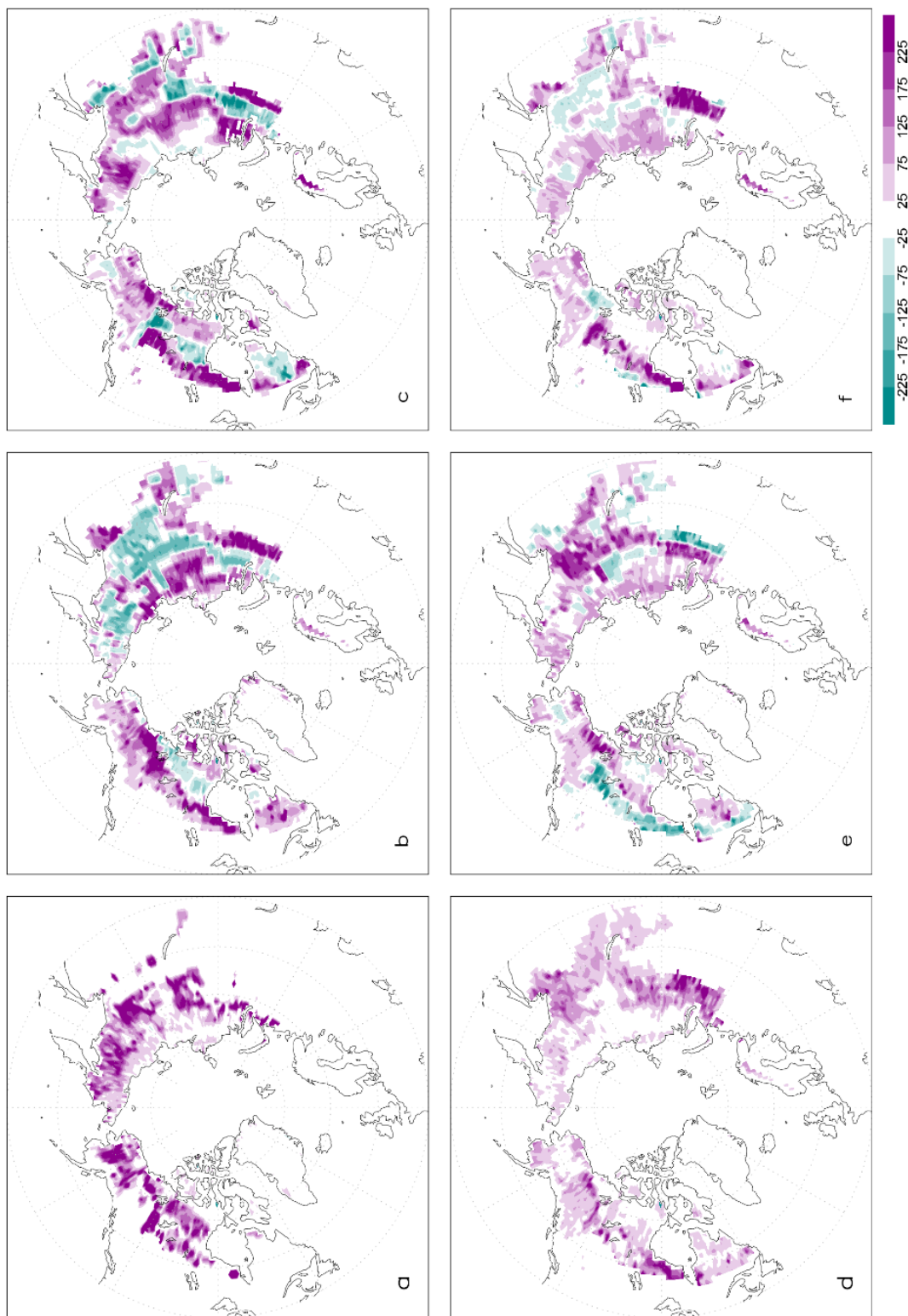


Figure 19. Same as Fig. 17, but for RCP 8.5 scenario

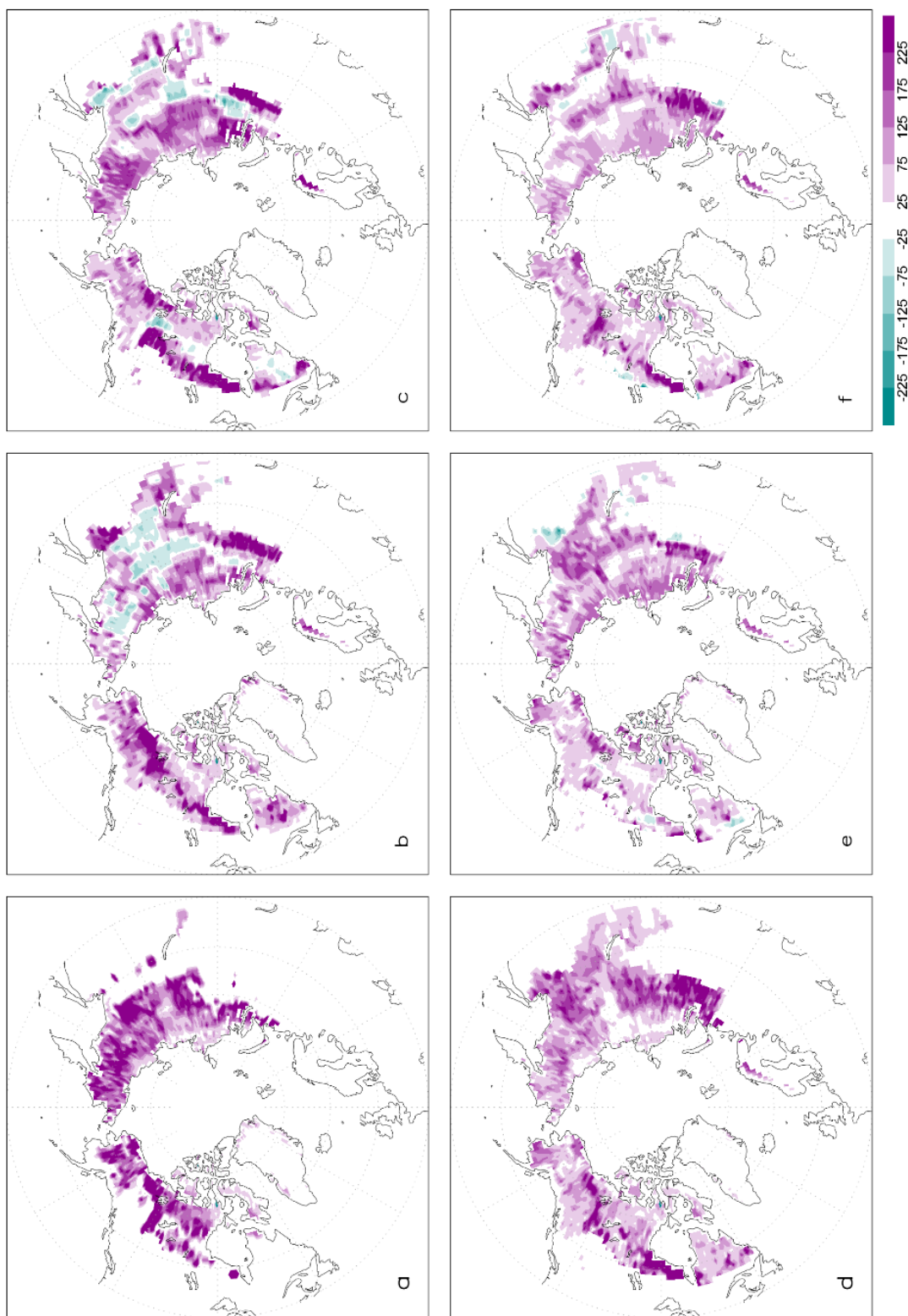


Figure 20. Same as Fig. 11, but for the 0.5% degradation rate.

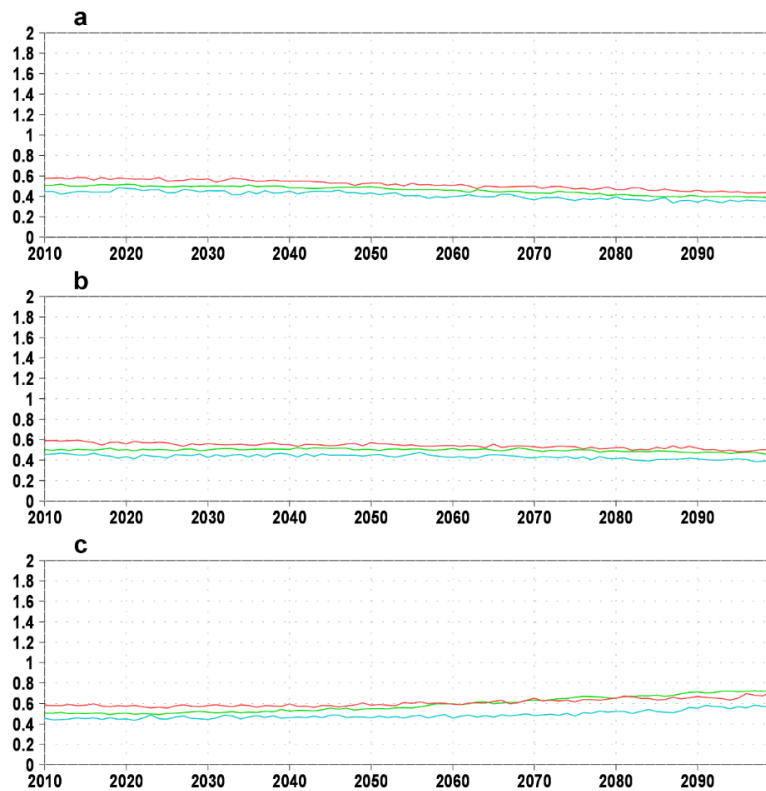
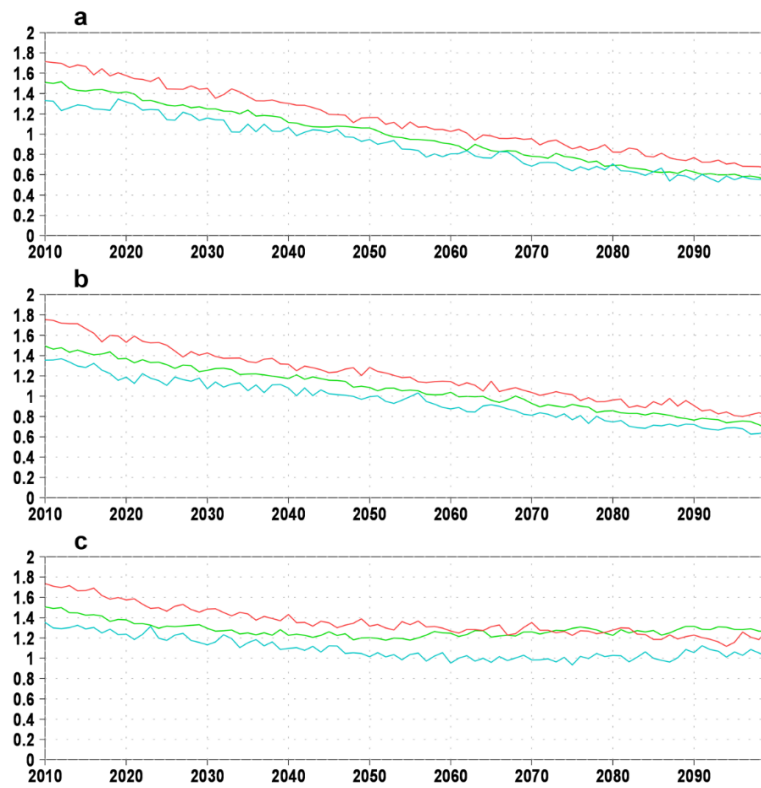


Figure 21. Same as Fig. 11, but for the 1.5% degradation rate.



GETTING IN TOUCH WITH THE EU

In person

All over the European Union there are hundreds of Europe Direct information centres. You can find the address of the centre nearest you at: https://europa.eu/european-union/contact_en

On the phone or by email

Europe Direct is a service that answers your questions about the European Union. You can contact this service:

- by freephone: 00 800 6 7 8 9 10 11 (certain operators may charge for these calls),
- at the following standard number: +32 22999696, or
- by electronic mail via: https://europa.eu/european-union/contact_en

FINDING INFORMATION ABOUT THE EU

Online

Information about the European Union in all the official languages of the EU is available on the Europa website at: https://europa.eu/european-union/index_en

EU publications

You can download or order free and priced EU publications from EU Bookshop at: <https://publications.europa.eu/en/publications>. Multiple copies of free publications may be obtained by contacting Europe Direct or your local information centre (see https://europa.eu/european-union/contact_en).

The European Commission's science and knowledge service

Joint Research Centre

JRC Mission

As the science and knowledge service of the European Commission, the Joint Research Centre's mission is to support EU policies with independent evidence throughout the whole policy cycle.



EU Science Hub
ec.europa.eu/jrc



@EU_ScienceHub



EU Science Hub - Joint Research Centre



EU Science, Research and Innovation



EU Science Hub



Publications Office
of the European Union

doi:10.2760/007066

ISBN 978-92-76-10182-6